

Posterior Label Smoothing for Node Classification

Jaeseung Heo¹, MoonJeong Park¹, Dongwoo Kim^{1, 2}

¹Graduate School of Artificial Intelligence, POSTECH, South Korea

²Department of Computer Science & Engineering, POSTECH, South Korea

jsheo12304@postech.ac.kr, mjeongp@postech.ac.kr, dongwookim@postech.ac.kr

Abstract

Label smoothing is a widely studied regularization technique in machine learning. However, its potential for node classification in graph-structured data, spanning homophilic to heterophilic graphs, remains largely unexplored. We introduce *posterior label smoothing*, a novel method for transductive node classification that derives soft labels from a posterior distribution conditioned on neighborhood labels. The likelihood and prior distributions are estimated from the global statistics of the graph structure, allowing our approach to adapt naturally to various graph properties. We evaluate our method on 10 benchmark datasets using eight baseline models, demonstrating consistent improvements in classification accuracy. The following analysis demonstrates that soft labels mitigate overfitting during training, leading to better generalization performance, and that pseudo-labeling effectively refines the global label statistics of the graph.

Code — <https://github.com/ml-postech/PosteL>

1 Introduction

Soft label, which contains class-wise probabilities, has demonstrated remarkable success in training neural networks across various domains, including computer vision and natural language processing (Lukov et al. 2022; Müller, Kornblith, and Hinton 2019; Szegedy et al. 2016; Vasudeva, Dolz, and Lombaert 2024; Vaswani et al. 2017; Zhang et al. 2021a). One of the popular approaches to obtain a soft label is label smoothing, which introduces uniform noise into the ground-truth labels. Despite its simplicity, this technique effectively regularizes the output distribution and enhances generalization (Pereyra et al. 2017). Knowledge distillation (Hinton, Vinyals, and Dean 2015) is another effective option, which trains a teacher model with a given one-hot label and utilizes its output as a soft-label to train the student model.

One of the most convincing explanations of why knowledge distillation works is that soft label enables the learning of “*dark knowledge*” included in instances (Allen-Zhu and Li 2023; Hinton, Vinyals, and Dean 2015). Since additional information captured by the teacher model that one-hot labels cannot convey is encoded as a soft label, the student model learns richer features.

Copyright © 2026, Association for the Advancement of Artificial Intelligence (www.aaai.org). All rights reserved.

Considering the graph dataset, the relation between nodes that the graph already contains can be helpful for node classification. As the quote says, “*You can tell a person by the company they keep*,” our idea is to encode the neighbor’s information into the soft label. More specifically, we utilize the posterior distribution, i.e., the probability of the node label given its neighbor nodes’ labels. This principle naturally generalizes both homophilic and heterophilic settings: in homophilic graphs, a target node is likely to have the same label as its neighbors, whereas in heterophilic graphs, the target node is likely to have different labels, which is supported by our theoretical analysis.

Existing approaches that generate soft labels in the graph domain build up the method based on a more specified assumption that nodes tend to share the same label with their neighboring nodes. Based on this assumption, they construct soft labels by naively aggregating the labels of neighboring nodes (Wang et al. 2021; Zhou et al. 2023). This approach aligns well with homophilic graphs, where nodes of the same class are likely to be connected, leading to improved generalization. However, it conflicts with the nature of heterophilic graphs, where edges frequently connect nodes with different labels.

Based on this intuition, we propose **Posterior Label Smoothing** (PosteL), a novel method that derives the soft label as the posterior distribution. The likelihood is approximated by the product of conditional label distributions over the node’s neighborhood. To estimate the prior and conditional distributions, we count label occurrences at nodes and label co-occurrences across edges, thereby constructing global statistics that capture the label dependencies encoded in the graph structure. The resulting soft label, therefore, encapsulates rich information from both the local neighborhood structure and the global label distribution.

Since PosteL needs the information of label co-occurrences and global statistics of the graph, accurate information would be important for the success of our approach. However, we can only access the labels of train nodes, while the labels of test nodes remain unknown. The lack of information can result in weakening the efficacy of our method. To address this issue, we propose an iterative pseudo-labeling procedure that utilizes pseudo-labels to re-obtain soft labels. Specifically, neighbor nodes’ information is updated and recalculated by the prior and likelihood,

which are also re-estimated by pseudo labels.

We apply our smoothing method to eight baseline neural network models, including a multi-layer perceptron and variants of graph neural networks, and test their performances on 10 graph benchmarks, including five homophilic and five heterophilic graphs. Across 80 model–dataset combinations, the soft label approach with iterative pseudo-labeling improves classification accuracy in 76 cases.

In summary, we make the following contributions:

- We propose a novel *posterior label smoothing* (PosteL) method that leverages local neighborhood structure and global adjacency statistics to derive soft labels.
- We prove that, under mild conditions, PosteL reflects the structural properties of the graph, particularly by preventing the soft label from being similar to the neighborhood labels in heterophilic graphs.
- We comprehensively evaluate PosteL on eight baseline neural network models and 10 graph datasets, achieving accuracy improvements in 76 of 80 model–dataset combinations.

2 Related Work

2.1 Node Classification

Various works leverage graph structures in different ways to perform node classification. Early approaches such as GCN (Kipf and Welling 2016), GraphSAGE (Hamilton, Ying, and Leskovec 2017), and GAT (Veličković et al. 2017) aggregate neighbor representations under the homophilic assumption. For tackling class imbalance on homophilic graphs, GraphSMOTE (Zhao, Zhang, and Wang 2021), Im-GAGN (Qu et al. 2021), and GraphENS (Park, Song, and Yang 2022) have been proposed. Meanwhile, H₂GCN (Zhu et al. 2020) and U-GCN (Jin et al. 2021) enhance performance on heterophilic graphs by aggregating representations from multi-hop neighbors. Other research focuses on adaptively learning the graph structure itself. For instance, GPR-GNN (Chien et al. 2020) and CPGNN (Zhu et al. 2021) determine which nodes to aggregate, while ChebNet (Defferrard, Bresson, and Vandergheynst 2016), APPNP (Gasteiger, Bojchevski, and Günnemann 2018), and BernNet (He et al. 2021) focus on learning appropriate filters from graph signals.

2.2 Classification with Soft Labels

Hinton, Vinyals, and Dean (2015) demonstrate that training a small student model with soft labels derived from a large teacher model’s predictions outperforms training with one-hot labels. This approach, known as knowledge distillation (KD), has proven effective for both model compression and performance improvement (Jiao et al. 2020; Liu et al. 2019; Tang and Wang 2018).

Alternatively, simpler methods for generating soft labels exist. Label smoothing (Szegedy et al. 2016) adds uniform noise to one-hot labels, and its benefits have been widely explored. For instance, Müller, Kornblith, and Hinton (2019) show that the label smoothing improves model calibration, while Lukasik et al. (2020) connect the label smoothing to

label-correction techniques and demonstrate its utility in addressing label noise. The label smoothing is popular in computer vision (Lukov et al. 2022; Vasudeva, Dolz, and Lombaert 2024; Zhang et al. 2021a) and NLP (Guo et al. 2021; Song et al. 2020; Vaswani et al. 2017), yet it remains relatively underexplored in the graph domain.

To our knowledge, only two studies specifically propose label smoothing techniques for node classification. SALs (Wang et al. 2021) smooths a node’s label to match those of its neighbors, and ALS (Zhou et al. 2023) aggregates neighborhood labels with adaptive refinements. However, neither work focuses on heterophilic graphs, where nodes often connect to dissimilar neighbors. Meanwhile, other studies have proposed smoothing the prediction output based on the graph structure (Xie, Kannan, and Kuo 2023; Zhang et al. 2021b), but their motivations differ substantially from the label smoothing approach investigated in this paper (e.g., they adjust output logits rather than training labels).

3 Method

In this section, we present our label smoothing approach for node classification and propose a new training strategy that iteratively refines soft labels via pseudo-labels obtained after training.

3.1 Posterior Label Smoothing

Let $\mathcal{G} = (\mathcal{V}, \mathcal{E}, \mathbf{X})$ be a graph, where \mathcal{V} is a set of nodes, and \mathcal{E} is a set of edges, and $\mathbf{X} \in \mathbb{R}^{|\mathcal{V}| \times d}$ is the d -dimensional node feature matrix. We consider a transductive node classification scenario in which we observe the graph structure for all nodes, including test nodes, but only the labels of nodes in the training set. For each node i in a training set, we have a label $y_i \in [K]$, where K is the total number of classes. Let $\mathbf{e}_i \in \{0, 1\}^K$ be a one-hot encoding of y_i , i.e., $e_{ik} = 1$ if $y_i = k$ and $\sum_k e_{ik} = 1$.

We propose an effective relabeling method to allocate a new soft label to each node based on the *local neighborhood structure* and *global label statistics*. Let \hat{Y}_i be a random variable representing the soft label of node i . Given the one-hop neighborhood $\mathcal{N}(i) = \{j \mid (i, j) \in \mathcal{E}\}$, we compute the posterior distribution of \hat{Y}_i conditioned on the labels of its neighbors using Bayes’ rule:

$$P(\hat{Y}_i = k \mid \{Y_j = y_j\}_{j \in \mathcal{N}(i)}) = \frac{P(\{Y_j = y_j\}_{j \in \mathcal{N}(i)} \mid \hat{Y}_i = k)P(\hat{Y}_i = k)}{\sum_{\ell=1}^K P(\{Y_j = y_j\}_{j \in \mathcal{N}(i)} \mid \hat{Y}_i = \ell)P(\hat{Y}_i = \ell)}. \quad (1)$$

To obtain the likelihood $P(\{Y_j = y_j\}_{j \in \mathcal{N}(i)} \mid \hat{Y}_i = k)$, we assume that the labels of the neighboring nodes are conditionally independent given \hat{Y}_i , i.e.,

$$P(\{Y_j\}_{j \in \mathcal{N}(i)} \mid \hat{Y}_i) = \prod_{j \in \mathcal{N}(i)} P(Y_j \mid \hat{Y}_i). \quad (2)$$

We empirically verify the conditional independence assumption in Section 5.2.

There are multiple ways to model the individual conditionals in the factorized form of Equation (2). In this work,

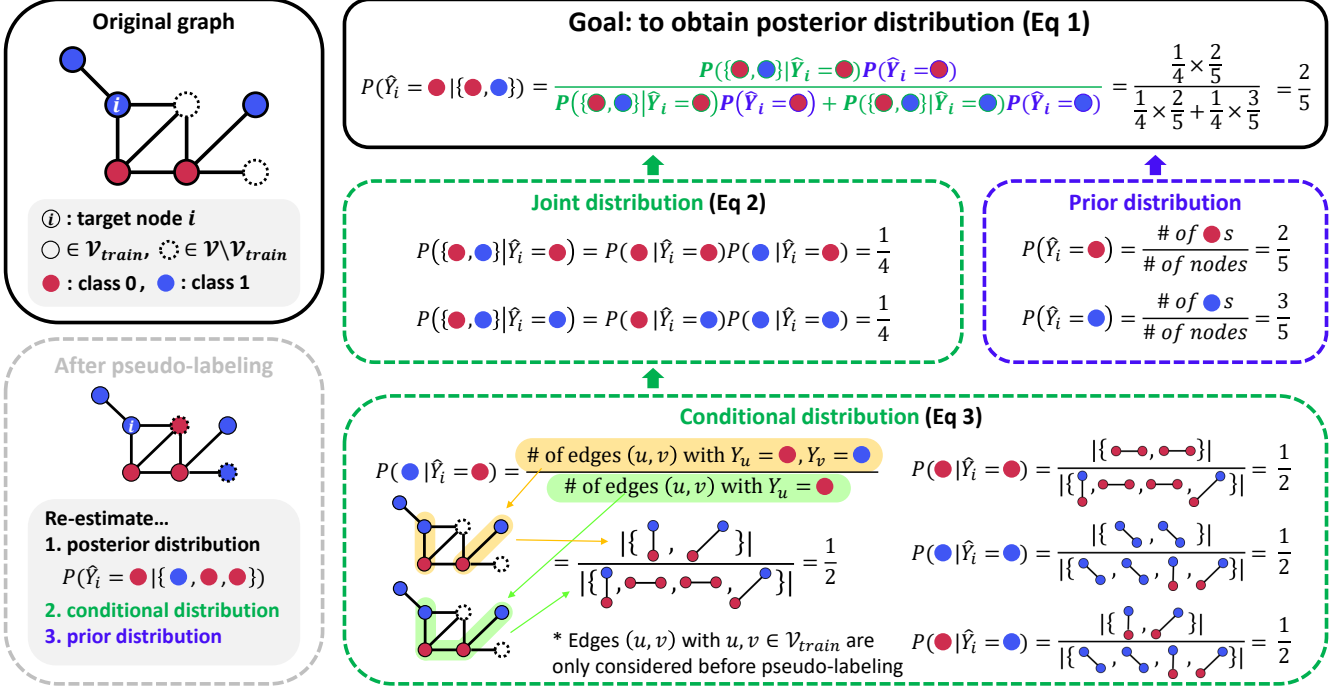


Figure 1: Overall illustration of posterior label smoothing. To relabel the node label, we compute the posterior distribution of the label given neighborhood labels. The likelihood and prior distributions are estimated from global statistics. The statistics are updated through the pseudo-labels after training, resulting in an iterative algorithm.

we use the global statistics between adjacent nodes to estimate the conditional. Specifically, we define

$$P(Y_j = m | \hat{Y}_i = n) := \frac{|\{(u, v) \mid y_v = m, y_u = n, (u, v) \in \mathcal{E}\}|}{|\{(u, v) \mid y_u = n, (u, v) \in \mathcal{E}\}|}. \quad (3)$$

We also estimate the prior distribution from global label frequencies. Concretely, we set $P(\hat{Y}_i = m) := |\{u \mid y_u = m\}|/|\mathcal{V}|$. In Appendix G, we investigate alternative designs for the likelihood and compare their performances. Figure 1 presents an example of obtaining the posterior distribution on a toy graph.

The posterior distribution serves as a soft label for model training. However, to prevent the posterior from becoming overly confident, we incorporate a small amount of uniform noise, ϵ . Additionally, because the most probable label from the posterior may not always align with the ground-truth, e.g., due to label noise or limited local information, we interpolate the posterior with the one-hot label. To this end, we obtain the target label $\hat{\mathbf{e}}_i$ used for actual training as

$$\hat{\mathbf{e}}_i = \alpha \tilde{\mathbf{e}}_i + (1 - \alpha) \mathbf{e}_i, \quad (4)$$

where $\tilde{e}_{ik} \propto P(\hat{Y}_i = k \mid \{Y_j = y_j\}_{j \in \mathcal{N}(i)}) + \beta \epsilon$, and α and β are hyperparameters controlling the weights of interpolation and uniform noise. By enforcing $\alpha < 1/2$, we can keep the most probable label of the target label the same as the ground-truth label, but we find that this condition is not necessary for empirical experiments. We refer to our method as

PosteL (**P**osterior **L**abel **s**mooothing). The detailed algorithm of PosteL is shown in Algorithm 1 in Appendix A.

3.2 Iterative Pseudo-labeling

Posterior relabeling derives a node's soft label by leveraging the labels of its neighbors. However, its effectiveness can be limited by certain graph properties, particularly sparsity and label noise. For instance, if a node has no labeled neighbors, the likelihood term becomes uniform, making the posterior depend solely on the prior; if only a few neighbors are labeled and those labels are noisy, the posterior can become skewed. These challenges are more pronounced in sparse graphs: in the Cornell dataset, for example, 26.35% of nodes have no labeled neighbors, making posterior relabeling especially difficult.

To address these limitations, we propose updating the likelihoods and priors using pseudo-labels generated for the validation and test nodes. Specifically, we first train a graph neural network with the target labels obtained from Equation (4) and then use its predictions on the validation and test nodes to obtain pseudo-labels. We assign each unlabeled node the most probable class from the model's output. Next, we update the likelihood and prior based on these pseudo-labels, while retaining the ground-truth labels for training nodes, to recalibrate both the posterior smoothing and the resulting soft labels.

We repeat this cycle of training and re-calibration until we achieve the best validation loss, aiming to maximize node classification performance. Intuitively, if posterior la-

bel smoothing improves predictive accuracy through better likelihood and prior estimation, then the resulting pseudo-labels should, in turn, further refine these distributions, provided that the pseudo-labels contain minimal errors. The detailed algorithms for the training process involving iterative pseudo-labeling are presented in Algorithm 2 in Appendix A.

4 Theoretical Analysis of PosteL

We analyze how PosteL behaves under different graph homophily and heterophily conditions in a binary classification setting. Specifically, we demonstrate how PosteL (i) adapts label assignments based on the neighborhood label distribution and (ii) remains robust across both homophilic and heterophilic graphs. While our focus here is on binary classification for clarity, a similar argument extends to multi-class scenarios as well.

Recall from Equation (3) that PosteL captures the adjacency relationship via empirical edge statistics. In the binary setting, let $\mathcal{N}_k(i)$ denote the set of neighbors of node i with label $k \in \{0, 1\}$. Further, we define the *class homophily* c_k for each label k as

$$c_k := \frac{|\{(i, j) \mid (i, j) \in \mathcal{E}, y_i = k, y_j = k\}|}{|\{(i, j) \mid (i, j) \in \mathcal{E}, y_i = k\}|}, \quad (5)$$

which measures how likely two adjacent nodes are both labeled k among all edges that include a node labeled k . Thus, $c_k > 0.5$ indicates that nodes labeled k tend to be adjacent to others with label k , i.e., *homophilic*, whereas $c_k < 0.5$ indicates they tend to connect to nodes with the opposite label, i.e., *heterophilic*.

The following lemma states the condition under which the posterior of label k is higher than $1 - k$.

Lemma 1 (Homophilic graph). *Suppose that the classes are balanced, i.e., $P(\hat{Y} = 0) = P(\hat{Y} = 1)$ and the graph is homophilic, i.e., $c_k > 1 - c_{1-k}$. Then, for any node i with neighbors $\mathcal{N}(i)$, the posterior probability satisfies,*

$$P(\hat{Y}_i = k \mid \{Y_j = y_j\}_{j \in \mathcal{N}(i)}) > 0.5$$

if and only if

$$|\mathcal{N}_k(i)| > |\mathcal{N}_{1-k}(i)| \cdot \frac{\log c_{1-k} - \log(1 - c_k)}{\log c_k - \log(1 - c_{1-k})}.$$

Intuitively, Lemma 1 states that if the graph is sufficiently homophilic, having more neighbors with label k than with label $1 - k$ pushes the posterior probability for k above 0.5.

A similar statement holds for heterophilic graphs.

Lemma 2 (Heterophilic graph). *Under the same assumptions used in Lemma 1, but now with a heterophilic condition, i.e., $c_k < 1 - c_{1-k}$, we have,*

$$P(\hat{Y}_i = k \mid \{Y_j = y_j\}_{j \in \mathcal{N}(i)}) > 0.5$$

if and only if

$$|\mathcal{N}_k(i)| < |\mathcal{N}_{1-k}(i)| \cdot \frac{\log c_{1-k} - \log(1 - c_k)}{\log c_k - \log(1 - c_{1-k})}.$$

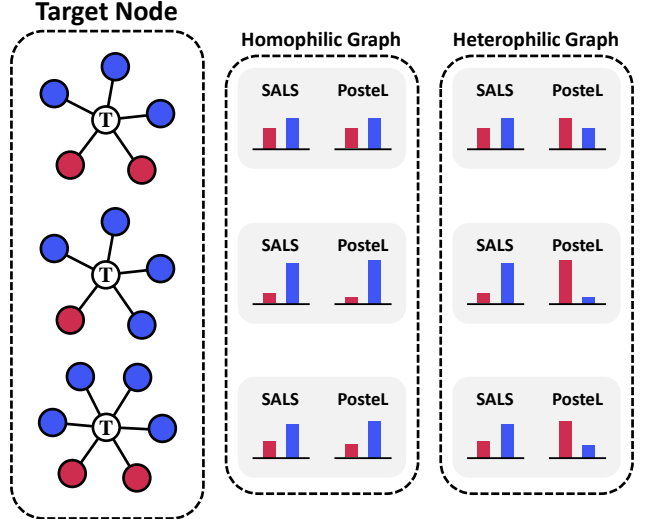


Figure 2: Toy example illustrating the difference between PosteL and SALS (Wang et al. 2021). The leftmost column shows three examples of a target node (represented as T) with different local neighborhood structures. The second and third columns show how SALS and PosteL create soft labels with homophilic and heterophilic graphs, respectively.

Lemma 2 indicates that in a heterophilic graph, having fewer neighbors of label k than of label $1 - k$ can make the posterior favor k . Detailed proofs are provided in Appendix B. These two lemmas highlight the key difference between PosteL and the neighborhood aggregation method in Wang et al. (2021). In their method, naively aggregating neighborhood labels for smoothing on heterophilic graphs results in the soft label being dominated by the majority neighborhood label. This *majority dominance* contradicts the inherent heterophilic property, where nodes are more likely to connect to dissimilar labels. In contrast, Lemma 2 demonstrates that PosteL assigns a lower probability to the majority neighborhood label in heterophilic graphs, thereby mitigating majority dominance, while Lemma 1 shows that PosteL effectively retains similarity to the majority neighbor label in homophilic graphs. Moreover, nodes in heterophilic graphs tend to connect with nodes that have different labels, which implies that $|\mathcal{N}_{y_i}(i)| < |\mathcal{N}_{1-y_i}(i)|$. In this case, PosteL preserves the ground-truth label as the most probable label. A similar effect is also found in homophilic graphs.

Additionally, we extend the previous results to accommodate the degrees of nodes with heterophilic graphs as follows.

Lemma 3 (Same degree). *With a balanced heterophilic graph where $0 < c_k < 0.5$, if two nodes n and m have the same degree d and $|\mathcal{N}_k(n)| > |\mathcal{N}_k(m)|$, then*

$$P(\hat{Y}_n = k \mid \{Y_j\}_{j \in \mathcal{N}(n)}) < P(\hat{Y}_m = k \mid \{Y_j\}_{j \in \mathcal{N}(m)}).$$

Lemma 3 shows that for nodes with the same degree, the posterior probability for a label k decreases as more neighbors share that label.

	Homophilic					Heterophilic				
	Cora	CiteSeer	PubMed	Computers	Photo	Chameleon	Actor	Squirrel	Texas	Cornell
GCN	87.14 \pm 1.01	79.86 \pm 0.67	86.74 \pm 0.27	83.32 \pm 0.33	88.26 \pm 0.73	59.61 \pm 2.21	33.23 \pm 1.16	46.78 \pm 0.87	77.38 \pm 3.28	65.90 \pm 4.43
+LS	87.77 \pm 0.97	81.06 \pm 0.59	87.73 \pm 0.24	89.08 \pm 0.30	94.05 \pm 0.26	64.81 \pm 1.53	33.81 \pm 0.75	49.53 \pm 1.10	77.87 \pm 3.11	67.87 \pm 3.77
+KD	87.90 \pm 0.90	80.97 \pm 0.56	87.03 \pm 0.29	88.56 \pm 0.36	93.64 \pm 0.31	64.49 \pm 1.38	33.33 \pm 0.78	49.38 \pm 0.64	78.03 \pm 2.62	63.61 \pm 5.57
+SALS	88.10 \pm 1.08	80.52 \pm 0.85	87.23 \pm 0.13	88.88 \pm 0.54	93.80 \pm 0.31	63.00 \pm 1.75	33.24 \pm 0.92	49.16 \pm 0.77	70.00 \pm 3.93	58.36 \pm 7.54
+ALS	88.10 \pm 0.85	81.02 \pm 0.52	87.30 \pm 0.30	89.18 \pm 0.36	93.88 \pm 0.27	64.11 \pm 1.29	34.05 \pm 0.49	47.44 \pm 0.76	77.38 \pm 2.13	71.64 \pm 3.28
+PosteL	88.56\pm0.90	82.10\pm0.50	88.00\pm0.25	89.30\pm0.23	94.08\pm0.35	65.80\pm1.23	35.16\pm0.43	52.76\pm0.64	80.82\pm2.79	80.33\pm1.80
Δ	+1.42(\uparrow)	+2.24(\uparrow)	+1.26(\uparrow)	+5.98(\uparrow)	+5.82(\uparrow)	+6.19(\uparrow)	+1.93(\uparrow)	+5.98(\uparrow)	+3.44(\uparrow)	+14.43(\uparrow)
GAT	88.03 \pm 0.79	80.52 \pm 0.71	87.04 \pm 0.24	83.32 \pm 0.39	90.94 \pm 0.68	63.13 \pm 1.93	33.93 \pm 2.47	44.49 \pm 0.88	80.82\pm2.13	78.21 \pm 2.95
+LS	88.69 \pm 0.99	81.27 \pm 0.86	86.33 \pm 0.32	88.95 \pm 0.31	94.06 \pm 0.39	65.16 \pm 1.49	34.55 \pm 1.15	45.94 \pm 1.60	78.69 \pm 4.10	74.10 \pm 4.10
+KD	87.47 \pm 0.94	80.79 \pm 0.60	86.54 \pm 0.31	88.99 \pm 0.46	93.76 \pm 0.31	65.14 \pm 1.47	35.13 \pm 1.36	43.86 \pm 0.85	79.02 \pm 2.46	73.44 \pm 2.46
+SALS	88.64 \pm 0.94	81.23 \pm 0.59	86.49 \pm 0.25	88.75 \pm 0.36	93.74 \pm 0.37	62.76 \pm 1.42	33.91 \pm 1.41	42.29 \pm 0.94	74.92 \pm 4.43	65.57 \pm 10.00
+ALS	88.60 \pm 0.92	81.09 \pm 0.68	87.06 \pm 0.24	89.57 \pm 0.35	94.16 \pm 0.36	66.15 \pm 1.25	34.05 \pm 0.52	46.85 \pm 1.45	78.03 \pm 3.11	75.08 \pm 3.77
+PosteL	89.21\pm1.08	82.13\pm0.64	87.08\pm0.19	89.60\pm0.29	94.31\pm0.31	66.28\pm1.14	35.92\pm0.72	49.38\pm1.05	80.33 \pm 2.62	80.33\pm1.81
Δ	+1.18(\uparrow)	+1.61(\uparrow)	+0.04(\uparrow)	+6.28(\uparrow)	+3.37(\uparrow)	+3.15(\uparrow)	+1.99(\uparrow)	+4.89(\uparrow)	-0.49(\downarrow)	+2.12(\uparrow)
BernNet	88.52 \pm 0.95	80.09 \pm 0.79	88.48 \pm 0.41	87.64 \pm 0.44	93.63 \pm 0.35	68.29 \pm 1.58	41.79\pm1.01	51.35 \pm 0.73	93.12 \pm 0.65	92.13 \pm 1.64
+LS	88.80 \pm 0.92	80.37 \pm 1.05	87.40 \pm 0.27	88.32 \pm 0.38	93.70 \pm 0.21	69.58 \pm 0.94	39.60 \pm 0.53	52.39 \pm 0.60	91.80 \pm 1.80	90.49 \pm 1.48
+KD	87.78 \pm 0.99	81.20 \pm 0.86	87.59 \pm 0.41	87.35 \pm 0.40	93.96 \pm 0.40	67.75 \pm 1.42	41.04 \pm 0.89	51.25 \pm 0.83	93.61 \pm 1.31	90.33 \pm 2.30
+SALS	88.77 \pm 0.85	81.20 \pm 0.61	88.61 \pm 0.35	88.87 \pm 0.33	94.22 \pm 0.43	64.62 \pm 0.85	40.15 \pm 1.07	46.19 \pm 0.78	85.90 \pm 4.10	88.03 \pm 3.12
+ALS	89.13 \pm 0.79	81.17 \pm 0.67	89.19\pm0.46	89.52 \pm 0.30	94.54\pm0.32	67.92 \pm 1.07	40.51 \pm 0.61	51.83 \pm 1.31	93.77 \pm 1.31	92.79 \pm 1.48
+PosteL	89.39\pm0.92	82.46\pm0.67	89.07 \pm 0.29	89.56\pm0.35	94.54\pm0.36	69.65\pm0.83	40.40 \pm 0.67	53.11\pm0.87	93.93\pm1.15	92.95\pm1.80
Δ	+0.87(\uparrow)	+2.37(\uparrow)	+0.59(\uparrow)	+1.92(\uparrow)	+0.91(\uparrow)	+1.36(\uparrow)	-1.39(\downarrow)	+1.76(\uparrow)	+0.81(\uparrow)	+0.82(\uparrow)

Table 1: Classification accuracy on 10 node classification datasets. Δ represents the performance improvement achieved by PosteL compared to the backbone model trained with the ground-truth label. All results of the backbone model trained with the ground-truth label are sourced from He et al. (2021).

Lemma 4 (Different degree). *With a balanced heterophilic graph where $0 < c_k < 0.5$, if there are two nodes n and m with degrees d_n and d_m such that $d_n > d_m$ and $|\mathcal{N}_k(n)| = |\mathcal{N}_k(m)|$, implying that $|\mathcal{N}_{1-k}(n)| > |\mathcal{N}_{1-k}(m)|$, then*

$$P(\hat{Y}_n = k \mid \{Y_j\}_{j \in \mathcal{N}(n)}) > P(\hat{Y}_m = k \mid \{Y_j\}_{j \in \mathcal{N}(m)}).$$

Lemma 4 highlights that for nodes with different degrees but the same number of neighbors labeled k , the posterior probability of k increases for nodes with more neighbors overall. This captures how higher connectivity amplifies the effect of dissimilar neighbors in heterophilic settings.

In Figure 2, we illustrate the difference between SALS (Wang et al. 2021) and PosteL with different levels of homophily. The first column shows three examples of a target node (represented as \top) with different local neighborhood structures. The second and third columns show how SALS and PosteL make soft labels with homophilic and heterophilic graphs, respectively. We visualize Lemma 3 through the heterophilic parts of the first and second graphs (rows) and Lemma 4 through the first and third graphs (rows). As the results indicate, both methods perform similarly in homophilic graphs but not in heterophilic ones. We note that the behavior of ALS (Zhou et al. 2023) is challenging to analyze due to the presence of the learnable component in their method. Except for the learnable part, the basic aggregation method of ALS is similar to that of SALS.

5 Experiments

The experimental section is composed of two parts. First, we evaluate the performance of our method for node classification through various datasets and models. Second, we pro-

vide a comprehensive analysis highlighting the importance of each design choice.

5.1 Node Classification

In this section, we evaluate the improvements in node classification performance achieved by our method across a range of datasets and backbone models. We aim to demonstrate the robustness and consistent effectiveness of our approach across graphs with varying structural and label characteristics.

Datasets We assess the performance of our method across 10 node classification datasets. To examine the effect of our method on diverse types of graphs, we conduct experiments on both homophilic and heterophilic graphs. For the homophilic setting, we evaluate our method on five datasets: Cora, CiteSeer, and PubMed, which are citation networks where nodes represent documents and edges correspond to citation links (Sen et al. 2008; Yang, Cohen, and Salakhudinov 2016), as well as the Amazon co-purchase graphs Computers and Photo (McAuley et al. 2015), where nodes represent products and edges indicate frequent co-purchases. For the heterophilic setting, we use five datasets: Chameleon and Squirrel, which are Wikipedia networks where nodes represent pages and edges correspond to mutual links (Rozemberczki, Allen, and Sarkar 2021); Actor, a co-occurrence network where nodes represent actors and edges indicate co-appearances on the same Wikipedia pages (Tang et al. 2009); and Texas and Cornell, which are webpage graphs where nodes represent web pages and edges denote hyperlinks (Pei et al. 2020). Detailed statistics of each dataset are illustrated in Appendix C.

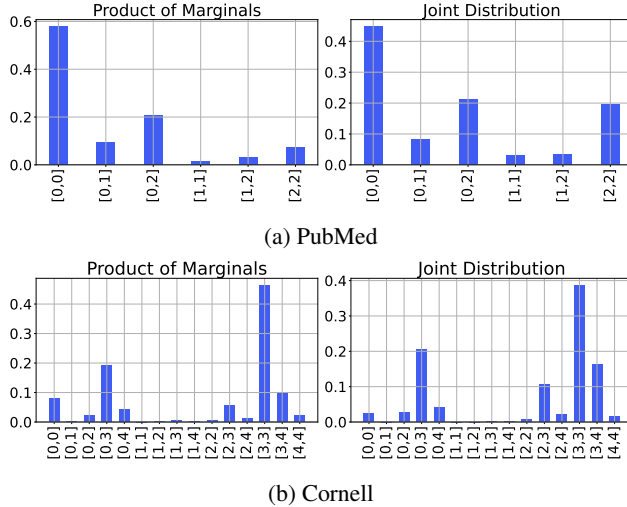


Figure 3: Estimated likelihood via product of marginals $P(Y_j|Y_i = 0, j \in \mathcal{N}(i)) \times P(Y_k|Y_i = 0, k \in \mathcal{N}(i))$ and empirical joint distribution $P(Y_j, Y_k|Y_i = 0, j, k \in \mathcal{N}(i))$.

Experimental Setup and Baselines We evaluate the performance of PosteL across various backbone models, including a multi-layer perceptron (MLP) without graph structure, and seven widely used graph neural networks: GCN (Kipf and Welling 2016), GAT (Veličković et al. 2017), APPNP (Gasteiger, Bojchevski, and Günnemann 2018), ChebNet (Defferrard, Bresson, and Vandergheynst 2016), GPR-GNN (Chien et al. 2020), BernNet (He et al. 2021), and OrderedGNN (Song et al. 2023).

We follow the experimental setup and backbone implementations of He et al. (2021). Specifically, we use fixed 10 sets of train, validation, and test splits with ratios of 60%/20%/20%, respectively, and measure the accuracy at the lowest validation loss. Each model is trained for 1,000 epochs, with early stopping applied if the validation loss does not improve over the last 200 epochs. Details of the experimental setup, including the hyperparameter search spaces and additional implementation specifics, are provided in Appendix D.

We compare our method with two domain-agnostic soft labeling methods, including label smoothing (LS) (Szegedy et al. 2016) and knowledge distillation (KD) (Hinton, Vinyals, and Dean 2015), as well as two label smoothing methods designed for node classification: SALS (Wang et al. 2021) and ALS (Zhou et al. 2023).

Results Table 1 reports the classification accuracy and 95% confidence intervals for each of the three models across ten datasets. Complete results, including the performance of APPNP, ChebNet, MLP, GPR-GNN, and OrderedGNN, are presented in Table 9 of Appendix G. Our method outperforms baseline methods in 76 out of 80 experimental settings. In 41 of these cases, the performance improvements exceed the 95% confidence interval, highlighting the robustness of our approach. On the Cornell dataset, using the GCN backbone, PosteL achieves a substantial improvement

of 14.43%.

Compared to other soft labeling methods, PosteL consistently achieves superior performance. In particular, our method outperforms SALS and ALS, which are label smoothing methods specifically tailored for node classification, on both homophilic and heterophilic datasets. The improvements are especially significant on heterophilic datasets, indicating that the heterophily-aware label assignment strategy of PosteL effectively enhances classification performance in heterophilic graph settings.

Nevertheless, on the Actor dataset, PosteL exhibits relatively weaker performance compared to other datasets. We provide an analysis of the reasons behind this weaker performance in Appendix E. In summary, on the Actor dataset, PosteL behaves similarly to uniform label smoothing due to nearly identical conditional distributions across different labels.

5.2 Empirical Analysis

In this section, we analyze the main experimental results from multiple perspectives, including validation of the conditional independence assumption, analysis of loss curves, and computational complexity. Further analyses provided in Appendix G include hyperparameter sensitivity, ablation studies, scalability to large-scale graphs, and comparisons of likelihood model design choices.

Empirical Validation of the Conditional Independence in Equation (2) In Equation (2), we approximate the joint conditional distribution of neighborhood labels using the product of individual conditional distributions. Although this factorization is exact when the neighborhood labels are conditionally independent given the central node’s label, this assumption is often violated in real-world datasets. To empirically validate our approximation, we compare the true joint distribution $P(Y_j = n, Y_k = m|Y_i = l)$ to the product of marginals $P(Y_j = n|Y_i = l) \times P(Y_k = m|Y_i = l)$. Figure 3 illustrates these distributions for the case $l = 0$. We observe that the product of marginals closely approximates the joint distribution, supporting the validity of our approximation.

Loss Curves Analysis We examine how soft labels affect GNN training dynamics by plotting the loss curves of GCN on the Squirrel dataset. Figure 4a compares the training, validation, and test losses when using ground-truth (GT) labels and PosteL labels. With PosteL, the gap between training loss and validation/test losses is noticeably smaller, indicating reduced overfitting. While the model trained with ground-truth labels begins to overfit after 50 epochs, PosteL remains stable through 200 epochs.

We hypothesize that correctly predicting PosteL labels, which encode local neighborhood information, enhances the model’s understanding of the graph structure and thereby improves generalization. Similar context-prediction strategies have been used as pretraining methods in previous studies (Hu et al. 2019; Rong et al. 2020). Loss curves for homophilic datasets are provided in Figure 9 and heterophilic in Figure 10 in Appendix G, showing consistent patterns across datasets.

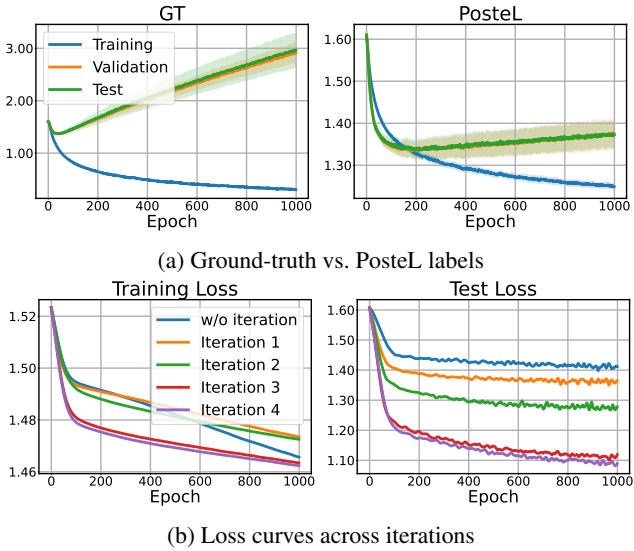


Figure 4: Loss curve comparisons: (a) using ground-truth (GT) labels versus PosteL labels on the Squirrel dataset; (b) across iterations of iterative pseudo-labeling on the Cornell dataset.

Effect of Iterative Pseudo-labeling We analyze the impact of iterative pseudo-labeling by examining the loss curves across iterations. Figure 4b shows the loss curves on the Cornell dataset, where test losses consistently decrease with each iteration. In this example, the model achieves its best performance after four iterations. On average, the best performance is observed at 1.13 iterations. The average number of iterations used to report the results in Table 9 is detailed in Appendix F.

Complexity Analysis The computational complexity of the posterior calculation is $O(|\mathcal{E}|K)$, which is negligible compared to the time complexity of a single pass through an L -layer GCN with fixed hidden dimension h , $O(L|\mathcal{E}|h + L|\mathcal{V}|h^2)$, since the posterior is computed once before training. The training time scales linearly with the number of pseudo-labeling iterations, but experiments show that an average of 1.13 iterations is sufficient, making our approach practical. A detailed complexity analysis can be found in Appendix F.

5.3 Posterior Estimation with Limited Labels

Our method estimates posterior probabilities from training set statistics. However, when training labels are limited, these estimated distributions may substantially deviate from the oracle distributions, potentially leading to inaccurate posterior probabilities. To examine this issue, we evaluate the quality of the estimated distributions using only 10% of the training data described in Section 5.1.

Figure 5 compares the conditional distributions on the Cornell dataset estimated using (1) training labels only, (2) training labels combined with pseudo-labels for validation and test nodes, and (3) all ground-truth labels. The con-

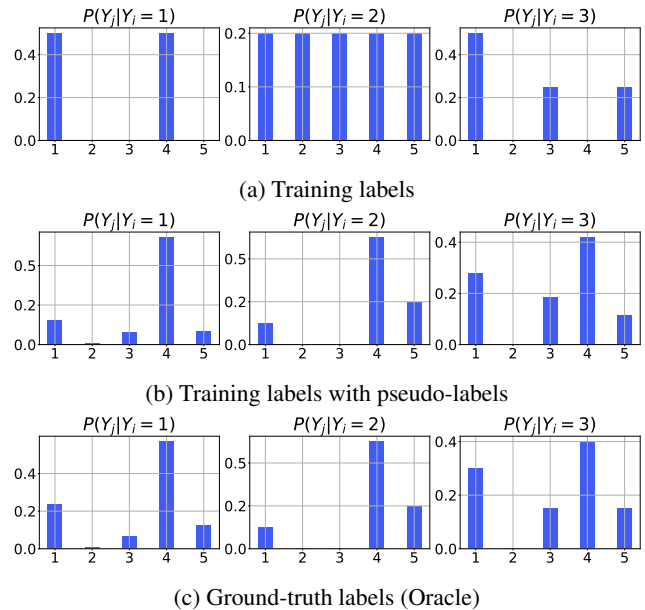


Figure 5: Estimated conditional distributions obtained from (a) training labels only, (b) training labels combined with pseudo-labels, and (c) all ground-truth labels.

	IPL	Cora	CiteSeer	Texas	Cornell
GCN	–	80.66±0.89	73.52±1.43	67.05±14.92	58.36±19.19
+PosteL	✗	81.59±1.23	74.97±1.62	69.67±14.76	64.59±15.25
+PosteL	✓	82.33±1.28	76.15±1.05	71.48±13.93	67.54±16.40

Table 2: Accuracy of the model trained with a limited training labels. The IPL column indicates whether iterative pseudo-labeling was applied: **✗** without IPL and **✓** with IPL.

ditional distributions estimated from limited training data show substantial deviation from the oracle distributions derived from all labels. In contrast, incorporating pseudo-labels reduces this discrepancy, yielding conditional distributions that closely match the oracle. We provide the same analysis on the other datasets in Appendix G.

Table 2 reports the classification accuracy of GCNs trained on 10% of the training data. Despite the limited availability of training labels, PosteL consistently enhances predictive accuracy. Particularly in the Texas and Cornell datasets, where pseudo-labeling substantially improves conditional distribution estimation, iterative pseudo-labeling achieves greater improvements compared to other datasets. This highlights the importance of refining conditional distributions to estimate posterior probabilities accurately.

6 Conclusion

We introduce a novel posterior label smoothing method for node classification on graphs. By combining local neighborhoods with global label statistics, PosteL improves model generalization. Extensive experiments on multiple datasets and models confirm its effectiveness, demonstrating significant performance gains over baseline methods.

Acknowledgements

We are grateful to Sangwoo Seo for providing insightful comments on this work. This work was supported by the National Research Foundation of Korea (NRF) grant funded by the Korea government(MSIT) (RS-2024-00337955; RS-2023-00217286) and Institute of Information & communications Technology Planning & Evaluation (IITP) grant funded by the Korea government(MSIT) (RS-2024-00457882, National AI Research Lab Project; RS-2019-II191906, Artificial Intelligence Graduate School Program(POSTECH)).

References

Allen-Zhu, Z.; and Li, Y. 2023. Towards Understanding Ensemble, Knowledge Distillation and Self-Distillation in Deep Learning. In *The Eleventh International Conference on Learning Representations*.

Chien, E.; Peng, J.; Li, P.; and Milenkovic, O. 2020. Adaptive universal generalized pagerank graph neural network. *arXiv preprint arXiv:2006.07988*.

Defferrard, M.; Bresson, X.; and Vandergheynst, P. 2016. Convolutional neural networks on graphs with fast localized spectral filtering. *Advances in neural information processing systems*, 29.

Gasteiger, J.; Bojchevski, A.; and Günnemann, S. 2018. Predict then propagate: Graph neural networks meet personalized pagerank. *arXiv preprint arXiv:1810.05997*.

Guo, B.; Han, S.; Han, X.; Huang, H.; and Lu, T. 2021. Label confusion learning to enhance text classification models. In *Proceedings of the AAAI conference on artificial intelligence*, volume 35, 12929–12936.

Hamilton, W.; Ying, Z.; and Leskovec, J. 2017. Inductive Representation Learning on Large Graphs. In Guyon, I.; Luxburg, U. V.; Bengio, S.; Wallach, H.; Fergus, R.; Vishwanathan, S.; and Garnett, R., eds., *Advances in Neural Information Processing Systems*, volume 30. Curran Associates, Inc.

He, M.; Wei, Z.; Xu, H.; et al. 2021. Bernnet: Learning arbitrary graph spectral filters via bernstein approximation. *Advances in Neural Information Processing Systems*, 34: 14239–14251.

Hinton, G.; Vinyals, O.; and Dean, J. 2015. Distilling the Knowledge in a Neural Network. In *NIPS Deep Learning and Representation Learning Workshop*.

Hu, W.; Fey, M.; Zitnik, M.; Dong, Y.; Ren, H.; Liu, B.; Catasta, M.; and Leskovec, J. 2020. Open graph benchmark: Datasets for machine learning on graphs. *Advances in neural information processing systems*, 33: 22118–22133.

Hu, W.; Liu, B.; Gomes, J.; Zitnik, M.; Liang, P.; Pande, V.; and Leskovec, J. 2019. Strategies for pre-training graph neural networks. *arXiv preprint arXiv:1905.12265*.

Jiao, X.; Yin, Y.; Shang, L.; Jiang, X.; Chen, X.; Li, L.; Wang, F.; and Liu, Q. 2020. TinyBERT: Distilling BERT for Natural Language Understanding. In *Findings of the Association for Computational Linguistics: EMNLP 2020*, 4163–4174. Association for Computational Linguistics.

Jin, D.; Yu, Z.; Huo, C.; Wang, R.; Wang, X.; He, D.; and Han, J. 2021. Universal Graph Convolutional Networks. In Beygelzimer, A.; Dauphin, Y.; Liang, P.; and Vaughan, J. W., eds., *Advances in Neural Information Processing Systems*.

Kipf, T. N.; and Welling, M. 2016. Semi-supervised classification with graph convolutional networks. *arXiv preprint arXiv:1609.02907*.

Liu, Y.; Chen, K.; Liu, C.; Qin, Z.; Luo, Z.; and Wang, J. 2019. Structured Knowledge Distillation for Semantic Segmentation. In *2019 IEEE/CVF Conference on Computer Vision and Pattern Recognition (CVPR)*, 2599–2608.

Lukasik, M.; Bhojanapalli, S.; Menon, A.; and Kumar, S. 2020. Does label smoothing mitigate label noise? In *International Conference on Machine Learning*, 6448–6458. PMLR.

Lukov, T.; Zhao, N.; Lee, G. H.; and Lim, S.-N. 2022. Teaching with soft label smoothing for mitigating noisy labels in facial expressions. In *European Conference on Computer Vision*, 648–665. Springer.

McAuley, J.; Targett, C.; Shi, Q.; and Van Den Hengel, A. 2015. Image-based recommendations on styles and substitutes. In *Proceedings of the 38th international ACM SIGIR conference on research and development in information retrieval*, 43–52.

Müller, R.; Kornblith, S.; and Hinton, G. E. 2019. When does label smoothing help? *Advances in neural information processing systems*, 32.

Park, J.; Song, J.; and Yang, E. 2022. GraphENS: Neighbor-Aware Ego Network Synthesis for Class-Imbalanced Node Classification. In *International Conference on Learning Representations*.

Pei, H.; Wei, B.; Chang, K. C.-C.; Lei, Y.; and Yang, B. 2020. Geom-gcn: Geometric graph convolutional networks. *arXiv preprint arXiv:2002.05287*.

Pereyra, G.; Tucker, G.; Chorowski, J.; Kaiser, Ł.; and Hinton, G. 2017. Regularizing neural networks by penalizing confident output distributions. *arXiv preprint arXiv:1701.06548*.

Qu, L.; Zhu, H.; Zheng, R.; Shi, Y.; and Yin, H. 2021. Imgagn: Imbalanced network embedding via generative adversarial graph networks. In *Proceedings of the 27th ACM SIGKDD Conference on Knowledge Discovery & Data Mining*, 1390–1398.

Rong, Y.; Bian, Y.; Xu, T.; Xie, W.; Wei, Y.; Huang, W.; and Huang, J. 2020. Self-supervised graph transformer on large-scale molecular data. *Advances in neural information processing systems*, 33: 12559–12571.

Rozemberczki, B.; Allen, C.; and Sarkar, R. 2021. Multi-scale attributed node embedding. *Journal of Complex Networks*, 9(2): cnab014.

Sen, P.; Namata, G.; Bilgic, M.; Getoor, L.; Galligher, B.; and Eliassi-Rad, T. 2008. Collective classification in network data. *AI magazine*, 29(3): 93–93.

Song, M.; Zhao, Y.; Wang, S.; and Han, M. 2020. Learning recurrent neural network language models with context-sensitive label smoothing for automatic speech recognition.

In *ICASSP 2020-2020 IEEE International Conference on Acoustics, Speech and Signal Processing (ICASSP)*, 6159–6163. IEEE.

Song, Y.; Zhou, C.; Wang, X.; and Lin, Z. 2023. Ordered gnn: Ordering message passing to deal with heterophily and over-smoothing. *arXiv preprint arXiv:2302.01524*.

Szegedy, C.; Vanhoucke, V.; Ioffe, S.; Shlens, J.; and Wojna, Z. 2016. Rethinking the Inception Architecture for Computer Vision. In *Proceedings of the IEEE Conference on Computer Vision and Pattern Recognition (CVPR)*.

Tang, J.; Sun, J.; Wang, C.; and Yang, Z. 2009. Social influence analysis in large-scale networks. In *Proceedings of the 15th ACM SIGKDD international conference on Knowledge discovery and data mining*, 807–816.

Tang, J.; and Wang, K. 2018. Ranking Distillation: Learning Compact Ranking Models With High Performance for Recommender System. In *Proceedings of the 24th ACM SIGKDD International Conference on Knowledge Discovery & Data Mining*, KDD ’18, 2289–2298. New York, NY, USA: Association for Computing Machinery.

Van der Maaten, L.; and Hinton, G. 2008. Visualizing data using t-SNE. *Journal of machine learning research*, 9(11).

Vasudeva, S. A.; Dolz, J.; and Lombaert, H. 2024. GeoLS: Geodesic label smoothing for image segmentation. In *Medical Imaging with Deep Learning*, 468–478. PMLR.

Vaswani, A.; Shazeer, N.; Parmar, N.; Uszkoreit, J.; Jones, L.; Gomez, A. N.; Kaiser, L. u.; and Polosukhin, I. 2017. Attention is All you Need. In Guyon, I.; Luxburg, U. V.; Bengio, S.; Wallach, H.; Fergus, R.; Vishwanathan, S.; and Garnett, R., eds., *Advances in Neural Information Processing Systems*, volume 30. Curran Associates, Inc.

Veličković, P.; Cucurull, G.; Casanova, A.; Romero, A.; Lio, P.; and Bengio, Y. 2017. Graph attention networks. *arXiv preprint arXiv:1710.10903*.

Wang, Y.; Cai, Y.; Liang, Y.; Wang, W.; Ding, H.; Chen, M.; Tang, J.; and Hooi, B. 2021. Structure-aware label smoothing for graph neural networks. *arXiv preprint arXiv:2112.00499*.

Xie, T.; Kannan, R.; and Kuo, C.-C. J. 2023. Label efficient regularization and propagation for graph node classification. *IEEE transactions on pattern analysis and machine intelligence*.

Yang, Z.; Cohen, W.; and Salakhudinov, R. 2016. Revisiting semi-supervised learning with graph embeddings. In *International conference on machine learning*, 40–48. PMLR.

Zhang, C.-B.; Jiang, P.-T.; Hou, Q.; Wei, Y.; Han, Q.; Li, Z.; and Cheng, M.-M. 2021a. Delving Deep Into Label Smoothing. *IEEE Transactions on Image Processing*, 30: 5984–5996.

Zhang, W.; Yang, M.; Sheng, Z.; Li, Y.; Ouyang, W.; Tao, Y.; Yang, Z.; and Cui, B. 2021b. Node dependent local smoothing for scalable graph learning. *Advances in Neural Information Processing Systems*, 34: 20321–20332.

Zhao, T.; Zhang, X.; and Wang, S. 2021. Graphsmote: Imbalanced node classification on graphs with graph neural networks. In *Proceedings of the 14th ACM international conference on web search and data mining*, 833–841.

Zhou, K.; Choi, S.-H.; Liu, Z.; Liu, N.; Yang, F.; Chen, R.; Li, L.; and Hu, X. 2023. Adaptive label smoothing to regularize large-scale graph training. In *Proceedings of the 2023 SIAM International Conference on Data Mining (SDM)*, 55–63. SIAM.

Zhu, J.; Rossi, R. A.; Rao, A.; Mai, T.; Lipka, N.; Ahmed, N. K.; and Koutra, D. 2021. Graph neural networks with heterophily. In *Proceedings of the AAAI conference on artificial intelligence*, volume 35, 11168–11176.

Zhu, J.; Yan, Y.; Zhao, L.; Heimann, M.; Akoglu, L.; and Koutra, D. 2020. Beyond Homophily in Graph Neural Networks: Current Limitations and Effective Designs. In Larochelle, H.; Ranzato, M.; Hadsell, R.; Balcan, M.; and Lin, H., eds., *Advances in Neural Information Processing Systems*, volume 33, 7793–7804. Curran Associates, Inc.

A Algorithms Related to Iterative Pseudo-labeling

Algorithm 1 and Algorithm 2 present the detailed algorithms for PosteL using pseudo-labels and the training process involving iterative pseudo-labeling.

Algorithm 1: Posterior label smoothing using pseudo-labels

Require: The set of training nodes $\mathcal{V}_{\text{train}}$ and the set of nodes with pseudo-label $\mathcal{V}_{\text{pseudo}}$; the number of classes K ; one-hot encoding of node labels $\{\mathbf{e}_i\}_{i \in \mathcal{V}_{\text{train}} \cup \mathcal{V}_{\text{pseudo}}}$; and the hyperparameters α and β .

Ensure: The set of soft labels $\{\hat{\mathbf{e}}_i\}_{i \in \mathcal{V}_{\text{train}}}$.

Initialize the set of labeled nodes:

$$\mathcal{V}_{\text{labeled}} = \mathcal{V}_{\text{train}} \cup \mathcal{V}_{\text{pseudo}}.$$

Estimate prior distribution for $m \in [K]$:

$$P(\hat{Y}_i = m) = \sum_{u \in \mathcal{V}_{\text{labeled}}} e_{um} / |\mathcal{V}_{\text{labeled}}|.$$

Define the set of labeled neighbors for each node u :

$$\mathcal{N}_{\text{labeled}}(u) = \mathcal{N}(u) \cap \mathcal{V}_{\text{labeled}}.$$

Estimate the empirical conditional for $n, m \in [K]$:

$$\begin{aligned} P(Y_j = m | \hat{Y}_i = n) \\ \propto \sum_{u: u \in \mathcal{V}_{\text{labeled}}, y_u = n} \sum_{v \in \mathcal{N}_{\text{labeled}}(u)} e_{vm}. \end{aligned}$$

for each $i \in \mathcal{V}_{\text{train}}$ do

Approximate the likelihood:

$$\begin{aligned} P(\{Y_j = y_j\}_{j \in \mathcal{N}_{\text{labeled}}(i)} | \hat{Y}_i = k) \\ \approx \prod_{j \in \mathcal{N}_{\text{labeled}}(i)} P(Y_j = y_j | \hat{Y}_i = k). \end{aligned} \quad (6)$$

Compute posterior distribution using Equation (1):

$$P(\hat{Y}_i = k | \{Y_j = y_j\}_{j \in \mathcal{N}_{\text{labeled}}(i)}).$$

Add uniform noise:

$$\tilde{e}_{ik} \propto P(\hat{Y}_i = k | \{Y_j = y_j\}_{j \in \mathcal{N}_{\text{labeled}}(i)}) + \beta \epsilon.$$

Obtain the soft label: $\hat{\mathbf{e}}_i = \alpha \tilde{\mathbf{e}}_i + (1 - \alpha) \mathbf{e}_i$.

end for

B The Proof of the Lemmas

Lemma 5 (Homophilic graph). *Suppose that the classes are balanced, i.e., $P(\hat{Y} = 0) = P(\hat{Y} = 1)$ and the graph is homophilic, i.e., $c_k > 1 - c_{1-k}$. Then, for any node i with neighbors $\mathcal{N}(i)$, the posterior probability satisfies,*

$$P(\hat{Y}_i = k | \{Y_j = y_j\}_{j \in \mathcal{N}(i)}) > 0.5$$

if and only if

$$|\mathcal{N}_k(i)| > |\mathcal{N}_{1-k}(i)| \cdot \frac{\log c_{1-k} - \log(1 - c_k)}{\log c_k - \log(1 - c_{1-k})}.$$

Algorithm 2: Training algorithm with iterative pseudo-labeling

Require: The input graph $\mathcal{G} = (\mathcal{V}, \mathcal{E}, \mathbf{X})$; the set of training nodes $\mathcal{V}_{\text{train}}$ and test nodes $\mathcal{V}_{\text{test}}$, where $\mathcal{V}_{\text{train}} \cup \mathcal{V}_{\text{test}} = \mathcal{V}$; one-hot encoded training labels $\{\mathbf{e}_i\}_{i \in \mathcal{V}_{\text{train}}}$; and PosteL, as described in algorithm 1, along with its parameters K, α , and β .

Ensure: Trained GNN model f with pseudo-labeled nodes.

Initialize the pseudo-labeled node set: $\mathcal{V}_{\text{pseudo}} = \emptyset$.

Initialize pseudo-labels: $\{\mathbf{e}_i\}_{i \in \mathcal{V}_{\text{pseudo}}} = \emptyset$.

while validation loss is decreasing **do**

 Apply posterior label smoothing:

$$\begin{aligned} \{\hat{\mathbf{e}}_i\}_{i \in \mathcal{V}_{\text{train}}} &= \text{PosteL}(\mathcal{V}_{\text{train}}, \mathcal{V}_{\text{pseudo}}), \\ \{\mathbf{e}_i\}_{i \in \mathcal{V}_{\text{training}} \cup \mathcal{V}_{\text{pseudo}}} &= (K, \alpha, \beta). \end{aligned}$$

Train the GNN model f to predict soft labels for the training nodes $\{\hat{\mathbf{e}}_i\}_{i \in \mathcal{V}_{\text{train}}}$.

Obtain pseudo-labels $\{\bar{y}_i\}_{i \in \mathcal{V}_{\text{test}}}$ and their one-hot encodings $\{\bar{\mathbf{e}}_i\}_{i \in \mathcal{V}_{\text{test}}}$ for test nodes:

$$\{\bar{y}_i\}_{i \in \mathcal{V}_{\text{test}}} = \{\arg \max f(\mathcal{G})_i\}_{i \in \mathcal{V}_{\text{test}}}.$$

Update the pseudo-labeled node set: $\mathcal{V}_{\text{pseudo}} = \mathcal{V}_{\text{test}}$.

Update pseudo-labels: $\{\mathbf{e}_i\}_{i \in \mathcal{V}_{\text{pseudo}}} = \{\bar{\mathbf{e}}_i\}_{i \in \mathcal{V}_{\text{test}}}$.

end while

Lemma 6 (Heterophilic graph). *Under the same assumptions used in Lemma 5, but now with a heterophilic condition, i.e., $c_k < 1 - c_{1-k}$, we have,*

$$P(\hat{Y}_i = k | \{Y_j = y_j\}_{j \in \mathcal{N}(i)}) > 0.5$$

if and only if

$$|\mathcal{N}_k(i)| < |\mathcal{N}_{1-k}(i)| \cdot \frac{\log c_{1-k} - \log(1 - c_k)}{\log c_k - \log(1 - c_{1-k})}.$$

Proof. In binary classification, the conditional probabilities can be expressed in terms of class homophily c_k as follows:

$$\begin{aligned} P(Y_j = k | \hat{Y}_i = k) &= c_k, \\ P(Y_j = 1 - k | \hat{Y}_i = k) &= 1 - c_k. \end{aligned}$$

By substituting these conditional probabilities into Equation (1), the posterior probability of \hat{Y}_i is given by:

$$\begin{aligned} P(\hat{Y}_i = k | \{Y_j = y_j\}_{j \in \mathcal{N}(i)}) \\ = \frac{c_k^{|\mathcal{N}_i^k|} (1 - c_k)^{|\mathcal{N}_i^{1-k}|}}{c_k^{|\mathcal{N}_i^k|} (1 - c_k)^{|\mathcal{N}_i^{1-k}|} + c_{1-k}^{|\mathcal{N}_i^{1-k}|} (1 - c_{1-k})^{|\mathcal{N}_i^k|}}, \end{aligned} \quad (7)$$

$$P(\hat{Y}_i = 1 - k | \{Y_j = y_j\}_{j \in \mathcal{N}(i)})$$

$$= \frac{c_{1-k}^{|\mathcal{N}_i^{1-k}|} (1 - c_{1-k})^{|\mathcal{N}_i^k|}}{c_k^{|\mathcal{N}_i^k|} (1 - c_k)^{|\mathcal{N}_i^{1-k}|} + c_{1-k}^{|\mathcal{N}_i^{1-k}|} (1 - c_{1-k})^{|\mathcal{N}_i^k|}},$$

where $\mathcal{N}_i^k = \{y_j = k | j \in \mathcal{N}(i)\}$ and $\mathcal{N}_i^{1-k} = \{y_j = 1 - k | j \in \mathcal{N}(i)\}$.

The condition under which the posterior probability of the soft label \hat{Y}_i for k is higher than that for $1 - k$ is given by the inequality:

$$c_k^{|\mathcal{N}_i^k|} (1 - c_k)^{|\mathcal{N}_i^{1-k}|} > c_{1-k}^{|\mathcal{N}_i^{1-k}|} (1 - c_{1-k})^{|\mathcal{N}_i^k|}.$$

Taking the logarithm of both sides, the inequality expands as follows:

$$\begin{aligned} |\mathcal{N}_i^k| \log c_k + |\mathcal{N}_i^{1-k}| \log(1 - c_k) \\ > |\mathcal{N}_i^{1-k}| \log c_{1-k} + |\mathcal{N}_i^k| \log(1 - c_{1-k}). \end{aligned}$$

Rearranging terms yields:

$$\begin{aligned} |\mathcal{N}_i^k| (\log c_k - \log(1 - c_{1-k})) \\ > |\mathcal{N}_i^{1-k}| (\log c_{1-k} - \log(1 - c_k)). \end{aligned}$$

Finally, dividing through by $\log c_k - \log(1 - c_{1-k})$, assuming it is nonzero, we obtain the condition:

$$|\mathcal{N}_i^k| \begin{cases} > |\mathcal{N}_i^{1-k}| \cdot \frac{\log c_{1-k} - \log(1 - c_k)}{\log c_k - \log(1 - c_{1-k})}, & \text{if } c_k > 1 - c_{1-k}, \\ < |\mathcal{N}_i^{1-k}| \cdot \frac{\log c_{1-k} - \log(1 - c_k)}{\log c_k - \log(1 - c_{1-k})}, & \text{if } c_k < 1 - c_{1-k}. \end{cases} \quad (8)$$

Thus, the condition in Lemma 5 holds in the first case of Equation (8), while the condition in Lemma 6 holds in the second case of Equation (8). \square

Lemma 7 (Same degree). *With a balanced heterophilic graph where $0 < c_k < 0.5$, if two nodes n and m have the same degree d and $|\mathcal{N}_n^k| > |\mathcal{N}_m^k|$, then*

$$P(\hat{Y}_n = k \mid \{Y_j\}_{j \in \mathcal{N}(n)}) < P(\hat{Y}_m = k \mid \{Y_j\}_{j \in \mathcal{N}(m)}).$$

Proof. For binary node classification, let d_i denote the degree of node i . We can express $|\mathcal{N}_i^{1-k}|$ as $d_i - |\mathcal{N}_i^k|$. Substituting into Equation (7) gives:

$$\begin{aligned} P(\hat{Y}_i = k \mid \{Y_j = y_j\}_{j \in \mathcal{N}(i)}) \\ = \frac{c_k^{|\mathcal{N}_i^k|} (1 - c_k)^{d_i - |\mathcal{N}_i^k|}}{c_k^{|\mathcal{N}_i^k|} (1 - c_k)^{d_i - |\mathcal{N}_i^k|} + c_{1-k}^{d_i - |\mathcal{N}_i^k|} (1 - c_{1-k})^{|\mathcal{N}_i^k|}}. \quad (9) \end{aligned}$$

By substituting Equation (9) into the inequality we aim to prove and simplifying the denominator, we obtain:

$$\begin{aligned} c_k^{|\mathcal{N}_n^k|} (1 - c_k)^{d - |\mathcal{N}_n^k|} c_{1-k}^{d - |\mathcal{N}_m^k|} (1 - c_{1-k})^{|\mathcal{N}_m^k|} \\ < c_k^{|\mathcal{N}_m^k|} (1 - c_k)^{d - |\mathcal{N}_m^k|} c_{1-k}^{d - |\mathcal{N}_n^k|} (1 - c_{1-k})^{|\mathcal{N}_n^k|}. \end{aligned}$$

Simplifying this expression leads to the following inequality:

$$\begin{aligned} (c_k c_{1-k})^{|\mathcal{N}_n^k| - |\mathcal{N}_m^k|} \\ < ((1 - c_k) (1 - c_{1-k}))^{|\mathcal{N}_n^k| - |\mathcal{N}_m^k|}. \end{aligned}$$

Since $c_k < 1 - c_k$ and $c_{1-k} < 1 - c_{1-k}$, it follows that $(1 - c_k) (1 - c_{1-k}) > c_k c_{1-k}$. Additionally, since $|\mathcal{N}_n^k| > |\mathcal{N}_m^k|$, the inequality holds. \square

Lemma 8 (Different degree). *With a balanced heterophilic graph where $0 < c_k < 0.5$, if there are two nodes n and m with degrees d_n and d_m such that $d_n > d_m$ and $|\mathcal{N}_n^k| = |\mathcal{N}_m^k|$, implying that $|\mathcal{N}_{1-k}(n)| > |\mathcal{N}_{1-k}(m)|$, then*

$$P(\hat{Y}_n = k \mid \{Y_j\}_{j \in \mathcal{N}(n)}) > P(\hat{Y}_m = k \mid \{Y_j\}_{j \in \mathcal{N}(m)}).$$

Proof. Using Equation (9), we need to show:

$$\begin{aligned} & \frac{c_k^{|\mathcal{N}_n^k|} (1 - c_k)^{d_n - |\mathcal{N}_n^k|}}{c_k^{|\mathcal{N}_n^k|} (1 - c_k)^{d_n - |\mathcal{N}_n^k|} + c_{1-k}^{d_n - |\mathcal{N}_n^k|} (1 - c_{1-k})^{|\mathcal{N}_n^k|}} \\ & > \frac{c_k^{|\mathcal{N}_m^k|} (1 - c_k)^{d_m - |\mathcal{N}_m^k|}}{c_k^{|\mathcal{N}_m^k|} (1 - c_k)^{d_m - |\mathcal{N}_m^k|} + c_{1-k}^{d_m - |\mathcal{N}_m^k|} (1 - c_{1-k})^{|\mathcal{N}_m^k|}}. \end{aligned}$$

Given that $|\mathcal{N}_n^k| = |\mathcal{N}_m^k|$, we expand the inequality:

$$\begin{aligned} & \frac{(1 - c_k)^{d_n}}{c_k^{|\mathcal{N}_n^k|} (1 - c_k)^{d_n - |\mathcal{N}_n^k|} + c_{1-k}^{d_n - |\mathcal{N}_n^k|} (1 - c_{1-k})^{|\mathcal{N}_n^k|}} \\ & > \frac{(1 - c_k)^{d_m}}{c_k^{|\mathcal{N}_m^k|} (1 - c_k)^{d_m - |\mathcal{N}_m^k|} + c_{1-k}^{d_m - |\mathcal{N}_m^k|} (1 - c_{1-k})^{|\mathcal{N}_m^k|}}. \end{aligned}$$

By eliminating the denominators:

$$\begin{aligned} & c_k^{|\mathcal{N}_n^k|} (1 - c_k)^{d_n + d_m - |\mathcal{N}_n^k|} \\ & + c_{1-k}^{d_m - |\mathcal{N}_n^k|} (1 - c_k)^{d_n} (1 - c_{1-k})^{|\mathcal{N}_n^k|} \\ & > c_k^{|\mathcal{N}_m^k|} (1 - c_k)^{d_n + d_m - |\mathcal{N}_m^k|} \\ & + c_{1-k}^{d_n - |\mathcal{N}_m^k|} (1 - c_k)^{d_m} (1 - c_{1-k})^{|\mathcal{N}_m^k|}. \end{aligned}$$

Subtracting $c_k^{|\mathcal{N}_n^k|} (1 - c_k)^{d_n + d_m - |\mathcal{N}_n^k|}$ from both sides:

$$\begin{aligned} & c_{1-k}^{d_m - |\mathcal{N}_n^k|} (1 - c_k)^{d_n} (1 - c_{1-k})^{|\mathcal{N}_n^k|} \\ & > c_{1-k}^{d_n - |\mathcal{N}_m^k|} (1 - c_k)^{d_m} (1 - c_{1-k})^{|\mathcal{N}_m^k|}. \end{aligned}$$

Finally, we have:

$$(1 - c_k)^{d_n - d_m} > c_{1-k}^{d_n - d_m}.$$

Since $c_k, c_{1-k} < 0.5, 1 - c_k > c_{1-k}$. And given $d_n > d_m$, the inequality holds. \square

C Dataset Statistics

We provide detailed statistics and explanations about the dataset used for the experiments in Table 3 and the paragraphs below.

Cora, CiteSeer, and PubMed Each node represents a paper, and an edge indicates a reference relationship between two papers. The task is to predict the research subjects of the papers.

Computers and Photo Each node represents a product, and an edge indicates a high frequency of concurrent purchases of the two products. The task is to predict the product category.

Table 3: Statistics of the dataset utilized in the experiments.

Dataset	# nodes	# edges	# features	# classes
Cora	2,708	5,278	1,433	7
CiteSeer	3,327	4,552	3,703	6
PubMed	19,717	44,324	500	3
Computers	13,752	245,861	767	10
Photo	7,650	119,081	745	8
Chameleon	2,277	31,396	2,325	5
Actor	7,600	30,019	932	5
Squirrel	5,201	198,423	2,089	5
Texas	183	287	1,703	5
Cornell	183	277	1,703	5

Chameleon and Squirrel Each node represents a Wikipedia page, and an edge indicates a link between two pages. The task is to predict the monthly traffic for each page. We use the classification version of the dataset, where labels are converted by dividing monthly traffic into five bins.

Actor Each node represents an actor, and an edge indicates that two actors appear on the same Wikipedia page. The task is to predict the category of the actors.

Texas and Cornell Each node represents a web page from the computer science department of a university, and an edge indicates a link between two pages. The task is to predict the category of each web page as one of the following: student, project, course, staff, or faculty.

D Detailed Experimental Setup

In this section, we provide the computer resources and search space for hyperparameters. Our experiments are executed on AMD EPYC 7513 32-core Processor and a single NVIDIA RTX A6000 GPU with 48GB of memory.

D.1 Learning Hyperparameters

We largely follow the search space outlined in He et al. (2021):

- Learning Rate: $\{0.001, 0.002, 0.01, 0.05\}$
- Weight Decay: $\{0, 0.0005\}$
- Model Depth: All GNNs have 2 layers.
- Linear Layer Dropout: Fixed at 0.5.

D.2 Model-Specific Hyperparameters

- **GCN** (Kipf and Welling 2016)
 - 2 layers
 - Hidden dimension: 64
- **GAT** (Veličković et al. 2017)
 - 2 layers
 - 8 attention heads, each with hidden dimension 8
- **APPNP** (Gasteiger, Bojchevski, and Günnemann 2018)
 - 2-layer MLP for feature extraction

- Hidden dimension: 64
- Power iteration steps: 10
- Teleport probability: $\{0.1, 0.2, 0.5, 0.9\}$
- **MLP**
 - 2 layers
 - Hidden dimension: 64
- **ChebNet**
 - 2 layers
 - Hidden dimension: 32
 - 2 propagation steps
- **GPR-GNN** (Chien et al. 2020)
 - 2-layer MLP for feature extraction
 - Hidden dimension: 64
 - Random walk path length: 10
 - PPR teleport probability: $\{0.1, 0.2, 0.5, 0.9\}$
 - Dropout ratio (propagation layers): $\{0.0, 0.1, 0.2, 0.3, 0.4, 0.5, 0.6, 0.7, 0.8, 0.9\}$
- **BernNet** (He et al. 2021)
 - 2-layer MLP for feature extraction
 - Hidden dimension: 64
 - Polynomial approximation order: 10
 - Dropout ratio (propagation layers): $\{0.0, 0.1, 0.2, 0.3, 0.4, 0.5, 0.6, 0.7, 0.8, 0.9\}$

D.3 PosteL Hyperparameters

- Posterior Label Ratio α : $\{0.1, 0.2, 0.3, 0.4, 0.5, 0.6, 0.7, 0.8, 0.9, 1.0\}$
- Uniform Noise Ratio β : $\{0, 0.1, 0.2, 0.3, 0.4, 0.5, 0.6, 0.7, 0.8, 0.9\}$

These two parameters control the interpolation weight between the posterior and one-hot labels (α) and the magnitude of uniform noise added to the posterior (β).

E Influence of Conditional Label Distribution

In this section, we analyze the conditional label distributions and relate these observations to the behavior of PosteL. Figure 6 presents the conditional label distributions for three different datasets. On the PubMed and Cornell datasets, there are clear differences in conditional distributions depending on the target node’s label. Specifically, the PubMed dataset is known to exhibit homophily, meaning nodes with identical labels tend to connect more frequently, and its conditional distributions clearly reflect this characteristic. In contrast, the conditional distributions in the Actor dataset exhibit minimal variation across different target node labels. In such cases, the prior distribution tends to dominate the posterior, thereby reducing the informativeness of posterior estimates regarding neighborhood labels, potentially limiting the effectiveness of our approach. These findings align with the results in Table 9, which indicate that the performance improvements on the Actor dataset are smaller compared to those observed on the PubMed and Cornell datasets.

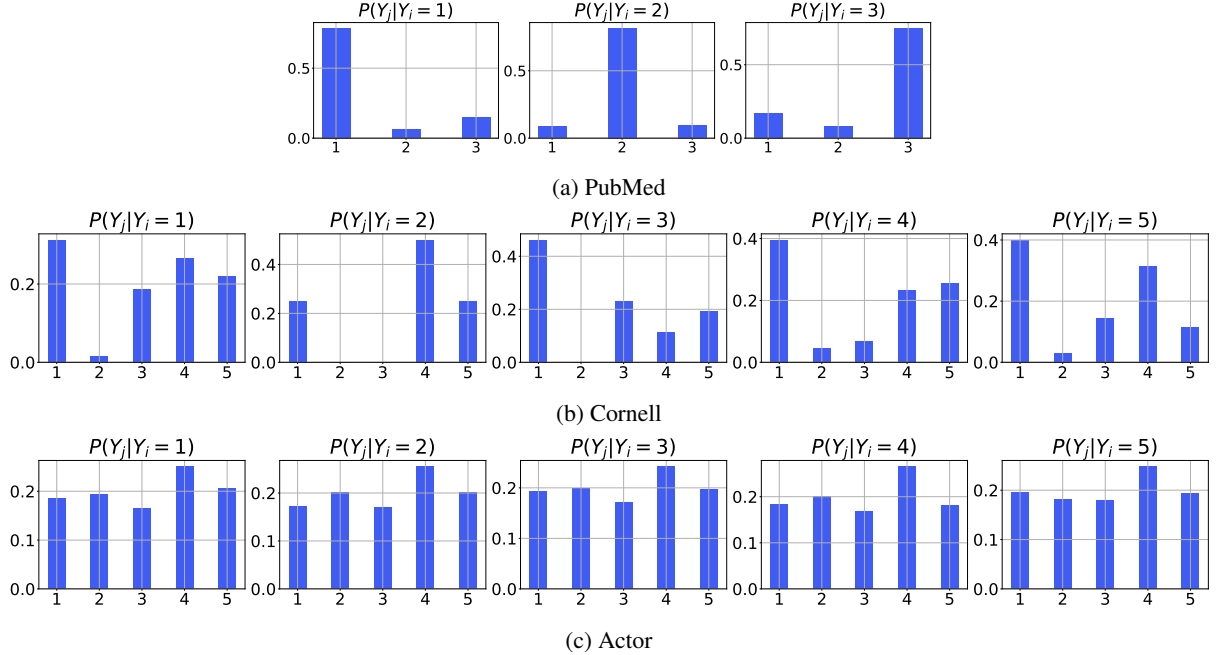


Figure 6: Empirical conditional distributions between two adjacent nodes. We omit the adjacent condition $(i, j) \in \mathcal{E}$ from the figures for simplicity.

F Complexity Analysis

In this section, we analyze the time complexity of Section 3.1 in detail. Specifically, we first show the complexities of deriving the prior and likelihood distributions independently, and then combine these results to determine the overall complexity of computing the posterior distribution.

First, the prior distribution $P(\hat{Y}_i = m)$ can be obtained as follows:

$$\hat{P}(Y_i = m) = \frac{|\{u \mid y_u = k\}|}{|\mathcal{V}|} = \frac{\sum_{u \in \mathcal{V}} e_{um}}{|\mathcal{V}|}. \quad (10)$$

The time complexity of calculating Equation (10) is $O(|\mathcal{V}|)$, so the time complexity of calculating the prior distribution for K classes is $O(|\mathcal{V}|K)$.

Next, calculating the empirical conditional $P(Y_j = m | \hat{Y}_i = n)$ from Equation (3) can be performed as follows:

$$P(Y_j = m | \hat{Y}_i = n) \propto \sum_{u: u \in \mathcal{V}, y_u = n} \sum_{v \in \mathcal{N}(u)} e_{vm}. \quad (11)$$

The time complexity of calculating Equation (11) for all possible pairs of m and n is $O(\sum_{u \in \mathcal{V}} |\mathcal{N}(u)|K)$. Since $\sum_{u \in \mathcal{V}} \mathcal{N}(u) = 2|\mathcal{E}|$, the time complexity for calculating empirical conditional is $O(|\mathcal{E}|K)$.

The likelihood is approximated through the product of empirical conditional distributions, denoted as $P(\{Y_j = y_j\}_{j \in \mathcal{N}(i)} | \hat{Y}_i = k) \approx \prod_{j \in \mathcal{N}(i)} P(Y_j = y_j | \hat{Y}_i = k)$. Likelihood calculation for all training nodes operates in $O(\sum_{u \in \mathcal{V}} |\mathcal{N}(u)|K)$ time complexity. So the overall computational complexity for likelihood calculation is $O(|\mathcal{E}|K)$.

After obtaining the prior distribution and likelihood, the posterior distribution is obtained by Bayes' rule in Equation (1). Applying Bayes' rule for $|\mathcal{V}|$ nodes and K classes can be done in $O(|\mathcal{V}|K)$. So the overall time complexity is $O(|\mathcal{E}| + |\mathcal{V}|)K$. In most cases, $|\mathcal{V}| < |\mathcal{E}|$, so the time complexity of PosteL is $O(|\mathcal{E}|K)$.

In Section 3.2, we introduce an iterative pseudo-labeling procedure that repeatedly refines the pseudo-labels of validation and test nodes to compute posterior labels. Because each iteration requires retraining the model from scratch, the number of iterations can become a significant bottleneck in terms of runtime. Consequently, we evaluate the iteration counts to assess this overhead. The average number of iterations for each backbone and dataset in Table 9 is presented in Table 4. With an overall mean iteration count of 1.13, we argue that this level of additional time investment is justifiable for the sake of performance enhancement.

Table 5 presents the average training times of PosteL and other baselines across all datasets in Section 5, using a GCN backbone. When iterative pseudo-labeling is employed, PosteL is approximately four times slower than using the ground-truth labels, while requiring a training time comparable to knowledge distillation and ALS. If this overhead is excessive, PosteL can be applied without iterative pseudo-labeling or with only a single pseudo-labeling iteration. In particular, PosteL without pseudo-labeling trains approximately three times faster than knowledge distillation and ALS, and one pseudo-labeling iteration is still faster than those methods while achieving comparable accuracy. Table 8 summarizes the accuracy results for each variant.

Table 4: Average iteration counts of iterative pseudo-labeling for each backbone and dataset used to report Table 9.

	Cora	CiteSeer	PubMed	Computers	Photo	Chameleon	Actor	Squirrel	Texas	Cornell
GCN+PosteL	2.5	2.2	1.5	1	0.9	0.9	1.1	0.7	1.8	2.5
GAT+PosteL	1.6	1.8	1	1.2	0.7	0.8	2	1.1	3.1	2.4
APPNP+PosteL	1.9	2	1.1	0.8	1.1	1	1.1	0.9	1.4	2.9
MLP+PosteL	1.7	2.2	0.4	0.7	0.7	0.1	0.8	0.6	0.9	2.4
ChebNet+PosteL	1.6	2.1	1.2	0.6	0.6	1	0.7	0.7	2	2
GPR-GNN+PosteL	0.8	1.1	0.8	0.5	1.3	1	0.3	0.7	1.1	1
BernNet+PosteL	1.5	1.8	0.9	0.8	1	1.5	1.5	0.5	1.2	2.1

Table 5: Overall training time for each smoothing method. PosteL (w/o) refers to PosteL without iterative pseudo-labeling, and PosteL (1) refers to PosteL with one iteration of pseudo-labeling.

	GCN	+LS	+KD	+SALS	+ALS	+PosteL	+PosteL (w/o)	+PosteL (1)
time (s)	0.83	0.84	3.54	0.90	2.87	3.38	1.08	1.94

G Additional Experiments

Hyperparameter Sensitivity Analysis Figure 7 shows the performance with varying values of α and β on GCN. The blue line indicates the performance with varying α , and the green line shows the performance with varying β . The red dotted line represents the performance with the ground-truth label. Regardless of the values of α and β , the performance consistently outperforms the case using ground-truth labels, indicating that PosteL is insensitive to α and β . We observe that α values greater than 0.8 may harm training, suggesting the necessity of interpolating ground-truth labels.

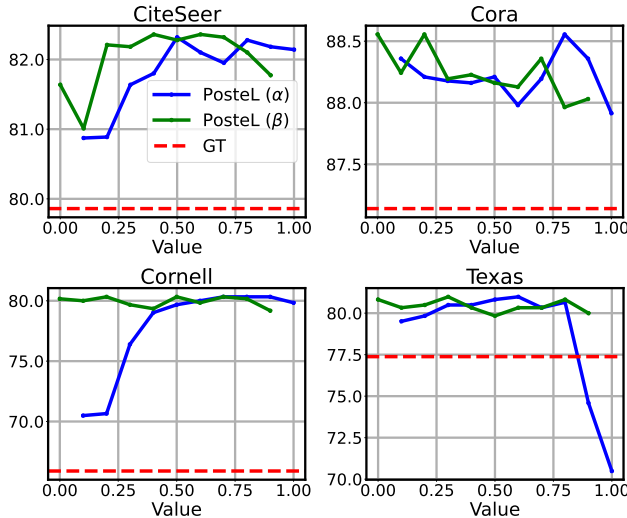


Figure 7: Hyperparameter sensitivity analysis on GCN.

Scalability to Large-scale Graphs We evaluated the runtime of PosteL on the ogbn-products dataset (Hu et al. 2020), which contains 2,449,029 nodes and 61,859,140 edges, to assess its computational efficiency on a large-scale graph. We measured the time excluding the training time for iterative pseudo-labeling. Generating soft labels with PosteL

takes 5.65 seconds, whereas a single training epoch requires 19.11 seconds, indicating that PosteL can generate soft labels efficiently even on large-scale graphs.

Table 6: The accuracy of label smoothing methods on the ogbn-products dataset using GCN.

	GCN	+LS	+SALS	+ALS	+PosteL
Products	80.62 \pm 0.68	80.99 \pm 0.50	81.12 \pm 0.13	80.46 \pm 0.38	81.20\pm0.68

Table 6 presents the performance of PosteL on the ogbn-products dataset using GCN. Although the improvement is not statistically significant, PosteL achieves the highest performance compared to other smoothing methods.

Design Choices of Likelihood Model We investigate alternative likelihood designs and introduce two PosteL variants: PosteL (normalized) and PosteL (local- H). In Equation (3), each edge equally contributes to the conditional probability, which can over-rely on high-degree nodes. To mitigate this, PosteL (normalized) adjusts edge contributions based on node degrees:

$$P^{\text{norm.}}(Y_j = m | \hat{Y}_i = n) := \frac{\sum_{y_u=n} \sum_{v \in \mathcal{N}(u)} \frac{1}{|\mathcal{N}(u)|} \cdot \mathbb{1}[y_v = m]}{|\{y_u = n \mid u \in \mathcal{V}\}|}, \quad (12)$$

where $\mathbb{1}$ is an indicator function.

In PosteL (local- H), likelihoods and priors are estimated from H -hop ego graphs, emphasizing local neighborhood statistics:

$$P^{\text{local-}H}(Y_j = m | \hat{Y}_i = n) := \frac{|\{(u, v) | y_v = m, y_u = n, (u, v) \in \mathcal{E}_i^{(H)}\}|}{|\{(u, v) | y_u = n, (u, v) \in \mathcal{E}_i^{(H)}\}|}, \quad (13)$$

where $\mathcal{E}_i^{(H)}$ is the set of edges in the H -hop neighborhood of node i , denoted as $\mathcal{N}^{(H)}(i)$. These variants allow us to

Table 7: Classification accuracy with various choices of likelihood model. PosteL (local-1) and (local-2) indicate that the likelihood is estimated within one- and two-hop neighbors of a target node, respectively. PosteL (norm.), shortened from PosteL (normalized), indicates that the likelihood is normalized based on the degree of a node.

	Cora	CiteSeer	Computers	Photo	Chameleon	Actor	Texas	Cornell
GCN	87.14 \pm 1.01	79.86 \pm 0.67	83.32 \pm 0.33	88.26 \pm 0.73	59.61 \pm 2.21	33.23 \pm 1.16	77.38 \pm 3.28	65.90 \pm 4.43
+PosteL (local-1)	88.26 \pm 1.07	81.42 \pm 0.46	89.08 \pm 0.31	93.61 \pm 0.40	65.36 \pm 1.25	33.48 \pm 1.03	79.02 \pm 3.11	71.97 \pm 4.10
+PosteL (local-2)	88.62 \pm 0.97	81.92 \pm 0.42	88.62 \pm 0.48	93.95 \pm 0.37	65.10 \pm 1.55	34.63 \pm 0.46	78.20 \pm 2.79	73.28 \pm 4.10
+PosteL (norm.)	89.00\pm0.99	81.86 \pm 0.70	89.30\pm0.39	94.13\pm0.39	66.00\pm1.14	34.90 \pm 0.63	80.33 \pm 2.95	80.00 \pm 1.97
+PosteL	88.56 \pm 0.90	82.10\pm0.50	89.30\pm0.23	94.08 \pm 0.35	65.80 \pm 1.23	35.16\pm0.43	80.82\pm2.79	80.33\pm1.80

Table 8: Ablation studies on three main components of PosteL on GCN. PS stands for posterior label smoothing, UN stands for uniform noise, and IPL stands for iterative pseudo-labeling. We use \checkmark to indicate the presence of the corresponding component in training and \times to indicate its absence. IPL with one indicates the performance with a single pseudo-labeling step.

PS	UN	IPL	Cora	CiteSeer	Computers	Photo	Chameleon	Actor	Texas	Cornell
\times	\times	\times	87.14 \pm 1.01	79.86 \pm 0.67	83.32 \pm 0.33	88.26 \pm 0.73	59.61 \pm 2.21	33.23 \pm 1.16	77.38 \pm 3.28	65.90 \pm 4.43
\checkmark	\times	\times	88.11 \pm 1.22	80.95 \pm 0.52	88.86 \pm 0.40	93.55 \pm 0.30	64.53 \pm 1.23	33.48 \pm 0.62	78.52 \pm 2.46	68.52 \pm 4.43
\times	\checkmark	\times	87.77 \pm 0.97	81.06 \pm 0.59	89.08 \pm 0.30	94.05 \pm 0.26	64.81 \pm 1.53	33.81 \pm 0.75	77.87 \pm 3.11	67.87 \pm 3.77
\checkmark	\times	\checkmark	88.56\pm0.90	81.64 \pm 0.57	88.70 \pm 0.27	93.70 \pm 0.37	64.25 \pm 1.93	34.71 \pm 0.76	80.82\pm2.79	80.16 \pm 1.97
\checkmark	\checkmark	\times	87.83 \pm 0.92	82.09 \pm 0.44	89.17 \pm 0.31	93.98 \pm 0.34	66.19\pm1.60	34.91 \pm 0.48	79.51 \pm 3.61	71.97 \pm 5.25
\checkmark	\checkmark	1	87.96 \pm 0.90	82.33\pm0.52	89.16 \pm 0.30	94.06 \pm 0.27	65.89 \pm 1.51	34.96 \pm 0.48	80.16 \pm 2.79	80.33\pm1.97
\checkmark	\checkmark	\checkmark	88.56\pm0.90	82.10 \pm 0.50	89.30\pm0.23	94.08\pm0.35	65.80 \pm 1.23	35.16\pm0.43	80.82\pm2.79	80.33\pm1.80

assess the importance of global versus local statistics in the smoothing process.

Table 7 shows the comparison between these variants. The likelihood with global statistics, e.g., PosteL and PosteL (normalized), performs better than the local likelihood methods, e.g., PosteL (local-1) and PosteL (local-2) in general, highlighting the importance of simultaneously utilizing global statistics. Especially in the Cornell dataset, a significant performance gap between PosteL and PosteL (local) is observed. PosteL (normalized) demonstrates similar performance to PosteL.

Ablation Studies We conduct ablation studies on three components of PosteL: posterior smoothing (PS), uniform noise (UN), and iterative pseudo-labeling (IPL), to evaluate their individual contributions. Table 8 summarizes the results.

The best performance is achieved when all components are included, highlighting their collective importance. IPL consistently improves performance across most datasets, especially Cornell, although omitting IPL still yields competitive results. Adding uniform noise further enhances performance on several datasets. Notably, PosteL surpasses using only uniform noise, a common label smoothing baseline.

Visualization of Node Embeddings Figure 8 presents the t-SNE (Van der Maaten and Hinton 2008) plots of node embeddings from the GCN with the Chameleon and Squirrel datasets. The node color represents the label. For each dataset, the left plot visualizes the embeddings with the ground-truth labels, while the right plot visualizes the embeddings with PosteL labels. The visualization shows that the embeddings from the soft labels form tighter clusters compared to those trained with the ground-truth labels. This

visualization results coincide with the t-SNE visualization of the previous work of Müller, Kornblith, and Hinton (2019).

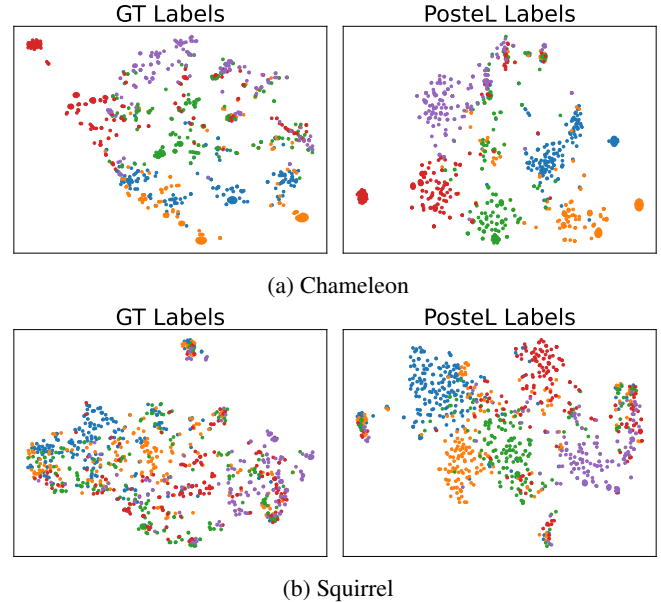


Figure 8: t-SNE plots of the final layer representation of the Chameleon and Squirrel datasets. For each dataset, the left figure displays the representations trained on the ground-truth labels, while the right figure displays the representations trained on the PosteL labels.

Extended Results of the Main Text We extend the experimental results presented in the main text to addi-

tional GNN backbones and datasets. Table 9 reports the classification accuracy for eight additional backbones, including APPNP (Gasteiger, Bojchevski, and Günnemann 2018), ChebNet (Defferrard, Bresson, and Vandergheynst 2016), MLP, GPR-GNN (Chien et al. 2020), and OrderedGNN (Song et al. 2023). Figures 9 and 10 show training/validation/test loss curves comparing ground-truth labels, SALS (Wang et al. 2021) labels, and PosteL labels on all 10 datasets used in our experiments. Figure 11 shows the estimated conditional distributions based on (i) training labels only, (ii) training labels combined with pseudo-labels, and (iii) all ground-truth labels.

	Homophilic						Heterophilic				
	Cora	CiteSeer	PubMed	Computers	Photo	Chameleon	Actor	Squirrel	Texas	Cornell	
GCN	87.14 \pm 1.01	79.86 \pm 0.67	86.74 \pm 0.27	83.32 \pm 0.33	88.26 \pm 0.73	59.61 \pm 2.21	33.23 \pm 1.16	46.78 \pm 0.87	77.38 \pm 3.28	65.90 \pm 4.43	
+LS	87.77 \pm 0.97	81.06 \pm 0.59	87.73 \pm 0.24	89.08 \pm 0.30	94.05 \pm 0.26	64.81 \pm 1.53	33.81 \pm 0.75	49.53 \pm 1.10	77.87 \pm 3.11	67.87 \pm 3.77	
+KD	87.90 \pm 0.90	80.97 \pm 0.56	87.03 \pm 0.29	88.56 \pm 0.36	93.64 \pm 0.31	64.49 \pm 1.38	33.33 \pm 0.78	49.38 \pm 0.64	78.03 \pm 2.62	63.61 \pm 5.57	
+SALS	88.10 \pm 1.08	80.52 \pm 0.85	87.23 \pm 0.13	88.88 \pm 0.54	93.80 \pm 0.31	63.00 \pm 1.75	33.24 \pm 0.92	49.16 \pm 0.77	70.00 \pm 3.93	58.36 \pm 7.54	
+ALS	88.10 \pm 0.85	81.02 \pm 0.52	87.30 \pm 0.30	89.18 \pm 0.36	93.88 \pm 0.27	64.11 \pm 1.29	34.05 \pm 0.49	47.44 \pm 0.76	77.38 \pm 2.13	71.64 \pm 3.28	
+PosteL	88.56\pm0.90	82.10\pm0.50	88.00\pm0.25	89.30\pm0.23	94.08\pm0.35	65.80\pm1.23	35.16\pm0.43	52.76\pm0.64	80.82\pm2.79	80.33\pm1.80	
Δ	+1.42(\uparrow)	+2.24(\uparrow)	+1.26(\uparrow)	+5.98(\uparrow)	+5.82(\uparrow)	+6.19(\uparrow)	+1.93(\uparrow)	+5.98(\uparrow)	+3.44(\uparrow)	+14.43(\uparrow)	
GAT	88.03 \pm 0.79	80.52 \pm 0.71	87.04 \pm 0.24	83.32 \pm 0.39	90.94 \pm 0.68	63.13 \pm 1.93	33.93 \pm 2.47	44.49 \pm 0.88	80.82\pm2.13	78.21 \pm 2.95	
+LS	88.69 \pm 0.99	81.27 \pm 0.86	86.33 \pm 0.32	88.95 \pm 0.31	94.06 \pm 0.39	65.16 \pm 1.49	34.55 \pm 1.15	45.94 \pm 1.60	78.69 \pm 4.10	74.10 \pm 4.10	
+KD	87.47 \pm 0.94	80.79 \pm 0.60	86.54 \pm 0.31	88.99 \pm 0.46	93.76 \pm 0.31	65.14 \pm 1.47	35.13 \pm 1.36	43.86 \pm 0.85	79.02 \pm 2.46	73.44 \pm 2.46	
+SALS	88.64 \pm 0.94	81.23 \pm 0.59	86.49 \pm 0.25	88.75 \pm 0.36	93.74 \pm 0.37	62.76 \pm 1.42	33.91 \pm 1.41	42.29 \pm 0.94	74.92 \pm 4.43	65.57 \pm 10.00	
+ALS	88.60 \pm 0.92	81.09 \pm 0.68	87.06 \pm 0.24	89.57 \pm 0.35	94.16 \pm 0.36	66.15 \pm 1.25	34.05 \pm 0.52	46.85 \pm 1.45	78.03 \pm 3.11	75.08 \pm 3.77	
+PosteL	89.21\pm1.08	82.13\pm0.64	87.08\pm0.19	89.60\pm0.29	94.31\pm0.31	66.28\pm1.14	35.92\pm0.72	49.38\pm1.05	80.33 \pm 2.62	80.33\pm1.81	
Δ	+1.18(\uparrow)	+1.61(\uparrow)	+0.04(\uparrow)	+6.28(\uparrow)	+3.37(\uparrow)	+3.15(\uparrow)	+1.99(\uparrow)	+4.89(\uparrow)	-0.49(\downarrow)	+2.12(\uparrow)	
APPNP	88.14 \pm 0.73	80.47 \pm 0.74	88.12 \pm 0.31	85.32 \pm 0.37	88.51 \pm 0.31	51.84 \pm 1.82	39.66 \pm 0.55	34.71 \pm 0.57	90.98 \pm 1.64	91.81 \pm 1.96	
+LS	89.01 \pm 0.64	81.58 \pm 0.61	88.90 \pm 0.32	87.28 \pm 0.27	94.34 \pm 0.23	53.98\pm1.47	39.44 \pm 0.78	36.81\pm0.98	91.31 \pm 1.48	89.51 \pm 1.81	
+KD	89.16 \pm 0.74	81.88 \pm 0.61	88.04 \pm 0.39	86.28 \pm 0.44	93.85 \pm 0.26	52.17 \pm 1.23	41.43\pm0.95	35.28 \pm 1.10	90.33 \pm 1.64	91.48 \pm 1.97	
+SALS	88.97 \pm 0.90	81.53 \pm 0.56	88.50 \pm 0.31	86.49 \pm 0.50	93.74 \pm 0.38	52.82 \pm 1.95	39.66 \pm 0.64	36.34 \pm 0.65	83.44 \pm 3.93	89.51 \pm 3.77	
+ALS	88.93 \pm 0.94	81.75 \pm 0.59	89.30\pm0.30	87.32 \pm 0.23	94.33 \pm 0.24	53.44 \pm 1.99	39.89 \pm 0.67	36.11 \pm 0.81	90.82 \pm 2.62	92.13 \pm 1.48	
+PosteL	89.62\pm0.84	82.47\pm0.66	89.17 \pm 0.26	87.46\pm0.29	94.42\pm0.24	53.83 \pm 1.66	40.18 \pm 0.70	36.71 \pm 0.60	92.13\pm1.48	93.44\pm1.64	
Δ	+1.48(\uparrow)	+2.00(\uparrow)	+1.05(\uparrow)	+2.14(\uparrow)	+5.91(\uparrow)	+1.99(\uparrow)	+0.52(\uparrow)	+2.00(\uparrow)	+1.15(\uparrow)	+1.63(\uparrow)	
MLP	76.96 \pm 0.95	76.58 \pm 0.88	85.94 \pm 0.22	82.85 \pm 0.38	84.72 \pm 0.34	46.85 \pm 1.51	40.19 \pm 0.56	31.03 \pm 1.18	91.45 \pm 1.14	90.82 \pm 1.63	
+LS	77.21 \pm 0.97	76.82 \pm 0.66	86.14 \pm 0.35	83.62 \pm 0.88	89.46 \pm 0.44	48.23 \pm 1.23	39.75 \pm 0.63	31.10 \pm 0.80	90.98 \pm 1.64	90.98 \pm 1.31	
+KD	76.32 \pm 0.94	77.75 \pm 0.75	85.10 \pm 0.29	83.89 \pm 0.53	88.23 \pm 0.38	47.40 \pm 1.75	41.32\pm0.75	32.58 \pm 0.83	89.34 \pm 1.97	91.80 \pm 1.15	
+SALS	77.29 \pm 1.05	77.00 \pm 0.90	85.78 \pm 0.33	82.55 \pm 0.51	89.11 \pm 0.52	43.68 \pm 1.69	39.47 \pm 0.73	30.88 \pm 0.68	86.39 \pm 5.09	89.11 \pm 0.52	
+ALS	77.59 \pm 0.69	77.24 \pm 0.82	86.43 \pm 0.43	84.26\pm0.66	89.86 \pm 0.43	48.03 \pm 1.38	39.98 \pm 0.94	31.33 \pm 0.89	91.64 \pm 3.44	91.64 \pm 1.31	
+PosteL	78.39\pm0.94	78.40\pm0.71	86.51\pm0.33	84.20 \pm 0.55	89.90\pm0.27	48.51\pm1.66	40.15 \pm 0.46	33.11\pm0.60	92.95\pm1.31	93.61\pm1.80	
Δ	+1.43(\uparrow)	+1.82(\uparrow)	+0.57(\uparrow)	+1.35(\uparrow)	+5.18(\uparrow)	+1.66(\uparrow)	-0.04(\downarrow)	+2.08(\uparrow)	+1.50(\uparrow)	+2.79(\uparrow)	
ChebNet	86.67 \pm 0.82	79.11 \pm 0.75	87.95 \pm 0.28	87.54 \pm 0.43	93.77 \pm 0.32	59.28 \pm 1.25	37.61 \pm 0.89	40.55 \pm 0.42	86.22 \pm 2.45	83.93 \pm 2.13	
+LS	87.22 \pm 0.99	79.70 \pm 0.63	88.48 \pm 0.29	89.55 \pm 0.38	94.53 \pm 0.37	66.41 \pm 1.16	39.39 \pm 0.73	42.55 \pm 1.11	87.21\pm2.62	84.59 \pm 2.30	
+KD	87.36 \pm 0.95	80.80 \pm 0.72	88.41 \pm 0.20	89.81 \pm 0.30	94.76 \pm 0.30	61.47 \pm 1.23	40.68\pm0.50	43.88 \pm 1.97	84.75 \pm 3.61	83.61 \pm 2.30	
+SALS	87.31 \pm 0.94	79.71 \pm 0.83	88.46 \pm 0.30	89.52 \pm 0.35	94.19 \pm 0.27	56.94 \pm 2.52	39.25 \pm 0.67	41.61 \pm 0.93	74.26 \pm 3.61	73.44 \pm 6.89	
+ALS	87.39 \pm 0.97	79.81 \pm 0.81	88.80 \pm 0.33	89.88 \pm 0.36	95.21\pm0.23	61.09 \pm 0.63	39.61 \pm 1.12	41.98 \pm 0.85	85.57 \pm 3.28	86.39 \pm 2.30	
+PosteL	88.57\pm0.92	82.48\pm0.52	89.20\pm0.31	89.95\pm0.40	94.87 \pm 0.25	66.83\pm0.77	39.56 \pm 0.51	50.87\pm0.90	86.39 \pm 2.46	88.52\pm2.63	
Δ	+1.90(\uparrow)	+3.37(\uparrow)	+1.25(\uparrow)	+2.41(\uparrow)	+1.10(\uparrow)	+7.55(\uparrow)	+1.95(\uparrow)	+10.32(\uparrow)	+0.17(\uparrow)	+4.59(\uparrow)	
GPR-GNN	88.57 \pm 0.69	80.12 \pm 0.83	88.46 \pm 0.33	86.85 \pm 0.25	93.85 \pm 0.28	67.28 \pm 1.09	39.92 \pm 0.67	50.15 \pm 1.92	92.95 \pm 1.31	91.37 \pm 1.81	
+LS	88.82 \pm 0.99	79.78 \pm 1.06	88.24 \pm 0.42	88.39 \pm 0.48	93.97 \pm 0.33	67.90 \pm 1.01	39.72 \pm 0.70	53.39 \pm 1.80	92.79 \pm 1.15	90.49 \pm 2.46	
+KD	89.33\pm1.03	81.24\pm0.85	89.85 \pm 0.56	87.88 \pm 1.11	94.23 \pm 0.51	66.76 \pm 1.31	42.00\pm0.63	53.26 \pm 1.07	94.26\pm1.48	88.52 \pm 1.97	
+SALS	88.78 \pm 0.90	80.71 \pm 0.91	90.12 \pm 0.46	88.63 \pm 0.35	94.23 \pm 0.65	65.16 \pm 1.49	39.67 \pm 0.73	44.75 \pm 1.45	73.61 \pm 3.44	82.46 \pm 2.95	
+ALS	88.93 \pm 1.31	80.31 \pm 0.71	90.23 \pm 0.50	89.14 \pm 0.48	94.55 \pm 0.53	67.79 \pm 1.07	40.09 \pm 0.72	51.34 \pm 1.00	92.95 \pm 1.31	89.18 \pm 2.13	
+PosteL	89.20 \pm 1.07	81.21 \pm 0.64	90.57\pm0.31	89.84\pm0.43	94.76\pm0.38	68.38\pm1.12	40.08 \pm 0.69	53.54\pm0.79	93.28 \pm 1.31	92.46\pm0.99	
Δ	+0.63(\uparrow)	+1.09(\uparrow)	+2.11(\uparrow)	+2.99(\uparrow)	+0.91(\uparrow)	+1.10(\uparrow)	+0.16(\uparrow)	+3.39(\uparrow)	+0.33(\uparrow)	+1.09(\uparrow)	
BernNet	88.52 \pm 0.95	80.09 \pm 0.79	88.48 \pm 0.41	87.64 \pm 0.44	93.63 \pm 0.35	68.29 \pm 1.58	41.79\pm1.01	51.35 \pm 0.73	93.12 \pm 0.65	92.13 \pm 1.64	
+LS	88.80 \pm 0.92	80.37 \pm 1.05	87.40 \pm 0.27	88.32 \pm 0.38	93.70 \pm 0.21	69.58 \pm 0.94	39.60 \pm 0.53	52.39 \pm 0.60	91.80 \pm 1.80	90.49 \pm 1.48	
+KD	87.78 \pm 0.99	81.20 \pm 0.86	87.59 \pm 0.41	87.35 \pm 0.40	93.96 \pm 0.40	67.75 \pm 1.42	41.04 \pm 0.89	51.25 \pm 0.83	93.61 \pm 1.31	90.33 \pm 2.30	
+SALS	88.77 \pm 0.85	81.20 \pm 0.61	88.61 \pm 0.35	88.87 \pm 0.33	94.22 \pm 0.43	64.62 \pm 0.85	40.15 \pm 1.07	46.19 \pm 0.78	85.90 \pm 4.10	88.03 \pm 3.12	
+ALS	89.13 \pm 0.79	81.17 \pm 0.67	89.19\pm0.46	89.52 \pm 0.30	94.54\pm0.32	67.92 \pm 1.07	40.51 \pm 0.61	51.83 \pm 1.31	93.77 \pm 1.31	92.79 \pm 1.48	
+PosteL	89.39\pm0.92	82.46\pm0.67	89.07 \pm 0.29	89.56\pm0.35	94.54\pm0.36	69.65\pm0.83	40.40 \pm 0.67	53.11\pm0.87	93.93\pm1.15	92.95\pm1.80	

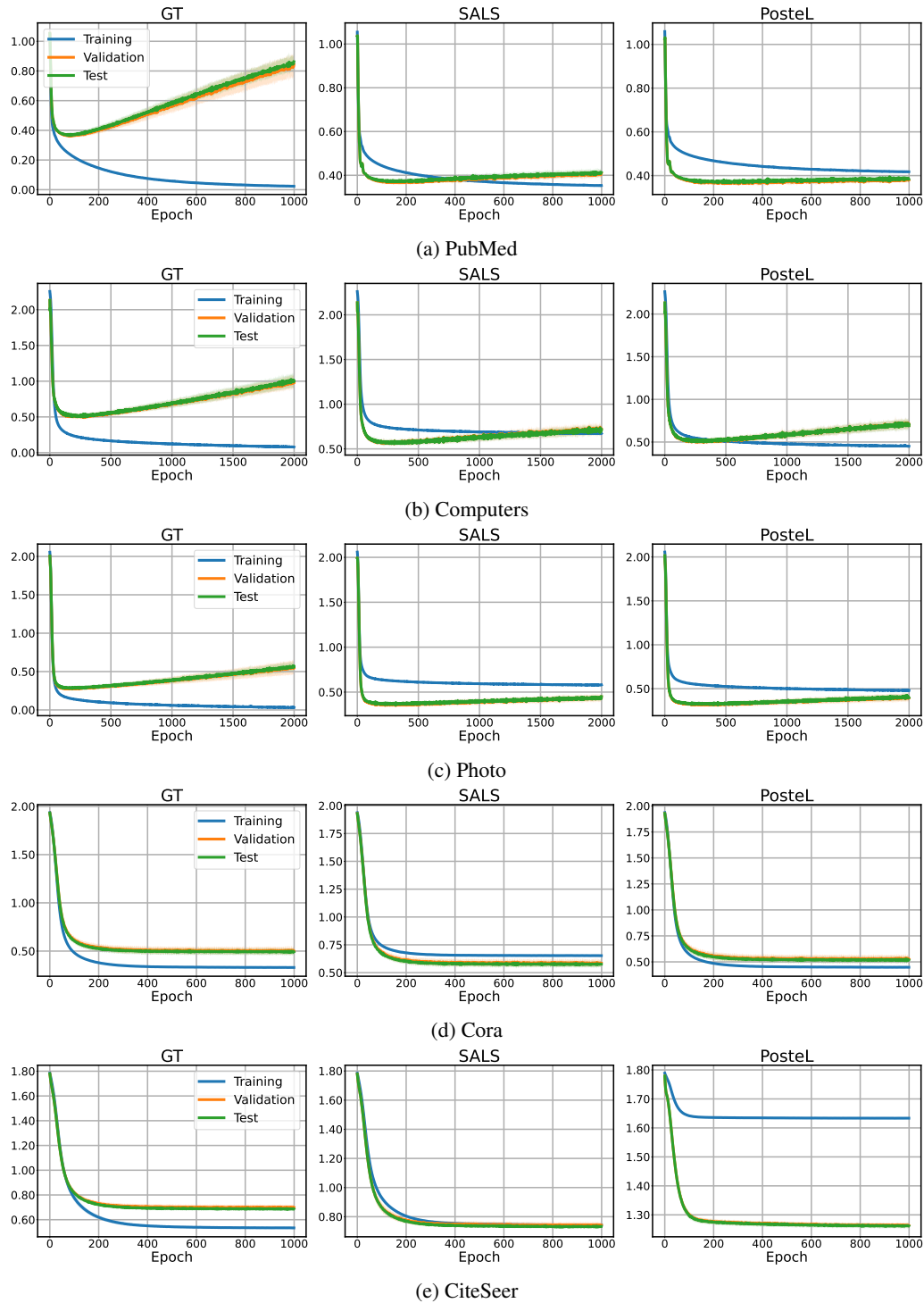


Figure 9: Loss curve of GCN trained on PosteL labels, SALS labels, and ground truth labels on homophilic datasets.

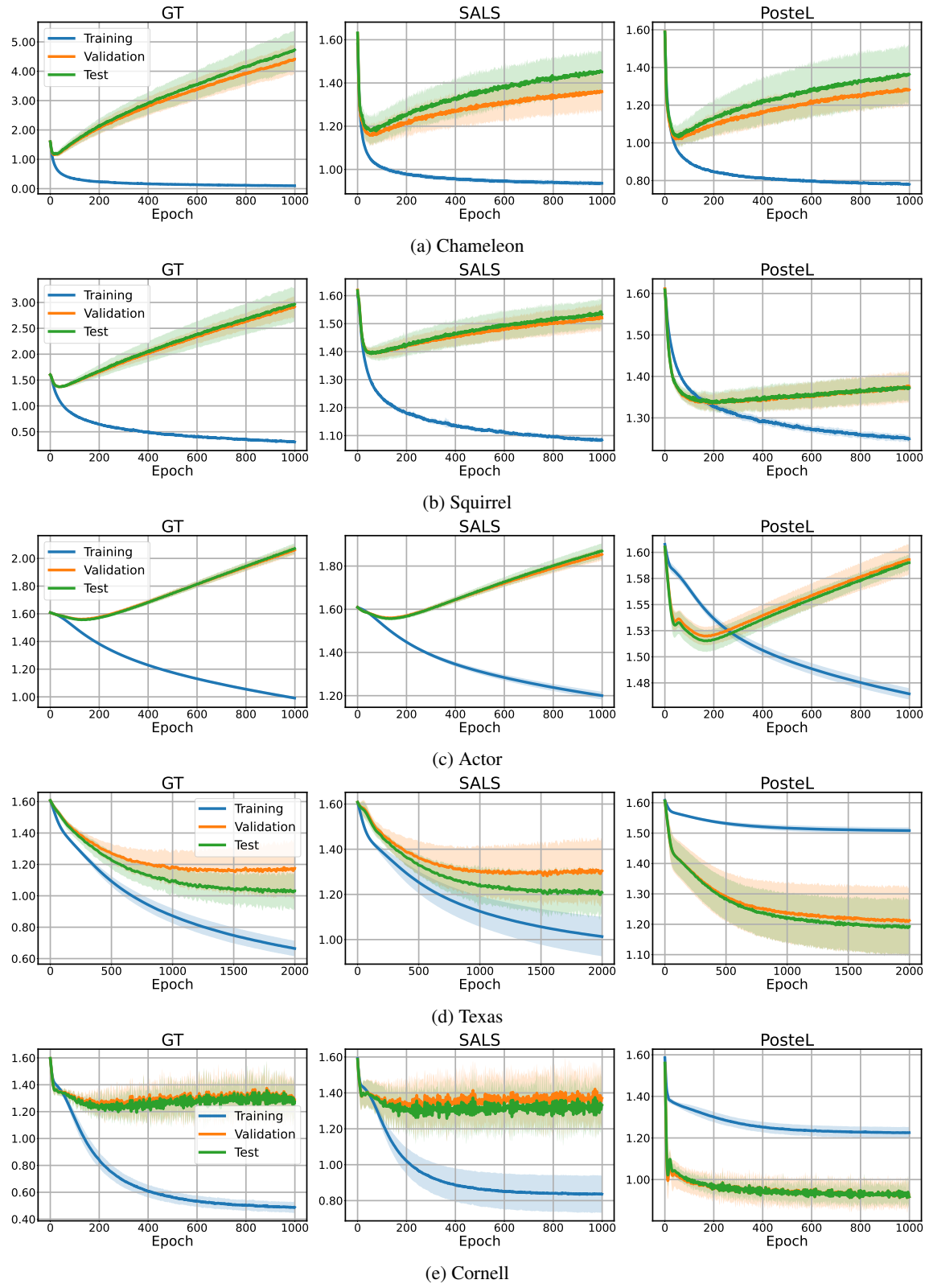


Figure 10: Loss curve of GCN trained on PosteL labels, SALS labels, and ground truth labels on heterophilic datasets.

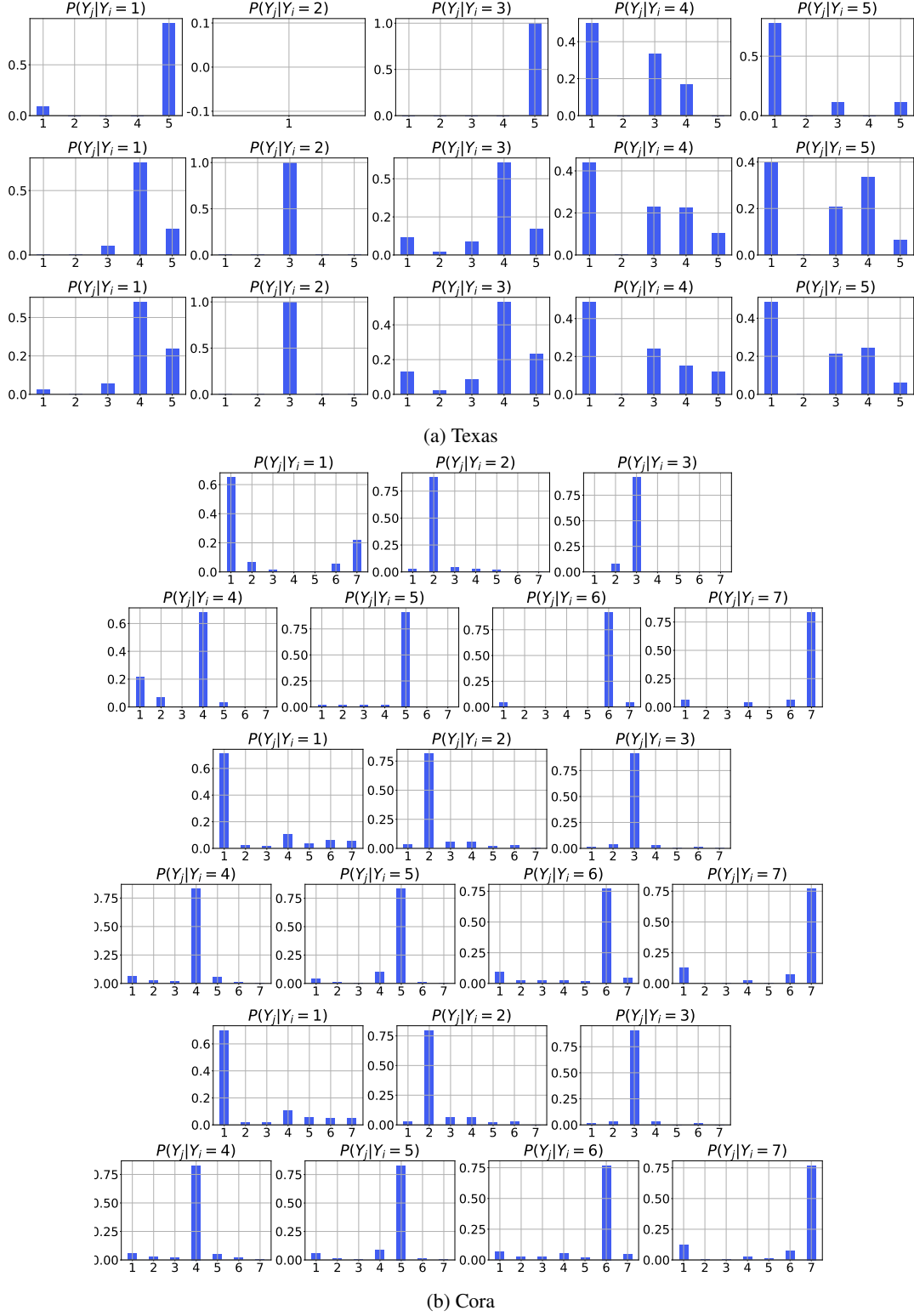


Figure 11: Estimated conditional distributions based on training labels only (top), training labels with pseudo-labels (middle), and all ground-truth labels (bottom).